Abstract

Five latitude surveys for measurements of the cosmic ray nucleonic and meson components have been carried out aboard M/S SOYA along a definite route between Japan and the Antarctic during 1956–1962. Using the data obtained from these surveys and also some other related data, investigations of the relationship between the cosmic ray intensity and the permanent magnetic field of the earth were performed, and the results are summarized in two parts.

In Part 1, latitude variations of cosmic ray intensities in a stationary state are studied with respect to the cosmic ray equator, the cosmic ray latitude knee, and the threshold rigidities. It is shown that the world-wide distribution of the cosmic ray neutron intensities at sea level is, in general, consistent with the spatial distribution of the vertical threshold rigidities determined from the trajectory calculations using a higher order simulation of the geomagnetic field. In this way, a table of the vertical threshold rigidities is prepared at 5° latitude and 10° longitude intervals. From comparisons of the threshold rigidities with experimental data, the overall uncertainty involved in the vertical threshold rigidity is found to be about 0.3 GV. This suggests the limitation of the usefulness of the vertical threshold rigidities which are supposed to account for the actual distribution of cosmic ray intensity over the globe. To minimize the uncertainty, it would be necessary to develope the study of the following three points: representation of the real geomagnetic field, correction for the penumbral effect, and influence of the inclined cosmic ray particles.

In Part 2, year-to-year change of the latitude variation of the cosmic ray intensity is examined throughout the last solar cycle 1954–1962. It is found that the position of the latitude knee moves toward a higher rigidity as solar activity increases, from about 1 GV at the solar minimum to about 3 GV at the solar maximum, whereas the geographical position of the cosmic-ray equator remains constant. The change in the slope of the intensity-rigitiy curve, indicating the change in the slope of the primary cosmic ray spectrum, appears to differ during the ascending and descending phases of the solar cycle. The 11-year variation of the response functions for the sea-level nucleonic component is deduced for every year, and is found to be consistent with PARKER's solar wind model proposed for interpretation of the solar cycle modulation. The threshold rigidities and the response functions presented would be available for analyses of other cosmic ray observation results. By actual application to the past special events such as the solar proton increase or the FORBUSH decrease, their general excellency and wide availability are established.

GENERAL INTRODUCTION

1. Geomagnetic effects

Cosmic ray particles coming to the earth are modulated systematically by the permanent magnetic field of the earth and occasionally by its time perturbation, resulting in intensity variations with geographic location and time. It is of great importance in this situation to accumulate more detailed experimental data on the world-wide distribution of the cosmic ray intensity, as well as to determine more precise values of rigidity of geomagnetic cutoff for cosmic ray particles. These two ways of investigations are complementary so that they should be developed always in parallel. Although it is necessary to study the active influence of the geomagnetic field on cosmic rays as a function of the radial distance from the earth's surface, the present study is limited to the problems directly concerned with cosmic ray modulations as observed on the ground level, in order to summarize the results from cosmic ray surveys performed at sea level during 1954–1962.

In measurements of the latitude effect of cosmic radiations, the nucleonic component played much more important role than the meson component which is subject to the temperature effect of the atmosphere. Also the fact that the amount of latitude change in the nucleonic component intensity is several times larger than that of the meson component is advantageous for the study. The first latitude survey for measurements of the nucleonic component was made by Rose *et al.* (1956) aboard the Labrador during the expedition voyage to the Arctic in 1954. Since then, a number of similar surveys were carried out by ships, trailers and aircrafts (Simpson, 1956; Simpson *et al.*, 1956; Katz *et al.*, 1958; Storey, 1959; Skorka, 1958; Pomerantz *et al.*, 1958; Pomerantz and Agarwal, 1962; Sandström *et al.*, 1963; Coxell *et al.*, 1966; Bachelet *et al.*, 1965; Carmichael *et al.*, 1965; Plooy *et al.*, 1963).

As one of the projects of the Japanese Antarctic Research Expedition, measurements of cosmic ray intensities have been carried out aboard the expedition ship Soya along a definite route between Japan and Syowa Station, Antarctica, five times during 1956–1962 (Fukushima *et al.*, 1963). Since this route happens to

pass through the two intense geomagnetic anomalies around Singapore and Cape Town, it seems to be advantageous for the study of higher term effects of the geomagnetic field on cosmic radiations. Other neutron data obtained from similar latitude surveys by various ships such as LABRADOR, ATKA, ARNEB and LEIPZIG, are utilized to supplement these data.

Another important matter in the research field related to cosmic ray surveys is the exact determination of the threshold rigidities effective for the cosmic ray particles reaching the different locations on the globe. Before about 1960, the geomagnetic study of the cosmic ray intensity was made generally in terms of the vertical threshold rigidity determined by analytical methods such as Störmer expression (for example, BARTELS, 1963; JORY, 1956; KODAMA *et al.*, 1957), QUENBY and WEBBER (1959), and QUENBY and WENK approximations (1962). In all of the cases, there remained a deviation of at least 1 GV in rigidity, even in the best case, when the rigidity spectra obtained at different longitudes were compared.

Meanwhile, KELLOGG (1960) pointed out that the cutoff rigidity near the equator, determined from trajectory calculations using a higher order expression for the geomagnetic field, is in good accord with observations at airplane altitudes. In addition, it was shown by FREON and MCCRACKEN (1962) that the threshold rigidity for Port auz Francais obtained from the same calculation favorably explains the rigidity spectrum of solar cosmic rays. Thus, such trajectory calculations have been developed rapidly for determination of cutoff rigidities in many other places on the earth by the help of high-speed computing machines (MCCRACKEN *et al.*, 1962; KODAMA, 1965; SHEA *et al.*, 1965a, b). In this work, further calculations are made not only for the ship positions but also for the improvements of the geographic distribution tables of the vertical threshold rigidities proposed by QUENBY and WEBBER, QUENBY and WENK, and MAKINO (1963). On the basis of the results of the above surveys and trajectory calculations, modulations of cosmic ray intensity in the vicinity of the geomagnetic field are discussed and summarized, taking into account the following three factors: 1) representation mode of the geomagnetic field simulation, 2) effect of cosmtic ray particles arriving from inclined directions and 3) penumbral effects.

2. Solar modulations

Studies of the change in the cosmic ray rigidity spectrum during the 11-year solar cycle should provide important clues to the mechanism of modulating the galactic cosmic radiation in the interplanetary space far from the vicinity of the geomagnetic field. It is believed that this problem may be closely related to a probable heliocentric magnetic field boundary (SIMPSON, 1962) and interplanetary magnetic irregularities (PARKER, 1958).

From an analysis of ionization chamber data from Huancayo, Cheltenham, Christchurch and Godhavn for a period between 1937 and 1952, FORBUSH (1954) showed that the mean level of cosmic ray intensity waxed and waned in anticor-

relation with solar activity, with an apparent period of 11 years. Continuous recording of cosmic ray intensity during the past decade by means of neutron monitors has considerably facilitated the study of the characteristics of this 11-year variation. It was found that at high latitudes the 11-year variation in the intensity of neutron components was 4 to 5 times greater than the corresponding variation in the intensity of ionizing component (FENTON *et al.*, 1958; MCCRACKEN and PARSONS, 1958). It became evident that the decrease of cosmic ray intensity lags behind the increase in solar activity by six to eight months (WEBBER, 1962; FORBUSH, 1958; FUKUSHIMA and KODAMA, 1961). FORBUSH (1958) and LOCKWOOD (1958, 1960) have pointed out that the largest decrease in the long term variation appears to occur after large FORBUSH decreases, the effects of which last for several months, followed by similar sharp decreases reducing the overall intensity further.

It is well known that an excellent method of obtaining the rigidity dependence of the 11-year variation makes use of the latitude variation measured at different times of the solar cycle with the same type of instrument. MEYER and SIMPSON (1955) monitored the cosmic ray intensity at an altitude of 30,000 feet over a definite route from the geomagnetic latitude 40°N to 60°N. STOREY (1960) recorded neutron intensity at an altitude of 20,000 feet during flights from Tasmania to New Guinea and back. MATHEWS and KODAMA (1964) compared the cosmic ray intensity recorded in different voyages by means of a shipborne neutron monitor. In all of these studies, data were compared for either of the period shorter than that of the 11-year variations, or the period between two extreme cases of the maximum solar activity and near the minimum. In this paper, details of year-to-year changes in the rigidity spectrum are analyzed and presented.

Another way of deducing the rigidity dependence of the long term variation was attempted by comparing the variations recorded by neutron monitors as different locations on the earth (MCCRACKEN, 1960; WEBBER, 1962). The data used were from a limited number of stations, and naturally the rigidity dependence over the entire range of rigidities of 1–15 GV could be obtained only by considerable extrapolations. Nevertheless, it is still worth comparing the results obtained by this method with those of the latitude surveys because from the former may be deduced the spectral change in time intervals arbitrary or shorter than by the latter.

In addition to the rigidity spectrum mentioned above, there are two interesting properties with respect to solar modulation of the latitude variation of cosmic ray intensity, *i. e.*, the cosmic ray equator and the latitude knee. The cosmic ray equator represents the integrated position of the magnetic field equator from the earth's surface out through the magnetosphere (SIMPSON *et al.*, 1956; CHERNOSKY *et al.*, 1964; ELLIOT and QUENBY, 1959). Accordingly a possible shift of the cosmic ray equator would be expected if the magnetosphere is modulated with the solar cycle. In ten sea level neutron monitor measurements made by

POMERANTZ *et al.* (1960) at 14°W during 1956–58, a maximum seasonal shift of 1.6° was found in the cosmic-ray equator. This fact is inconsistent with the result by KODAMA *et al.* (1962) that showed no solar cycle shift. Whereas, it is believed that the position of the latitude knee, indicating the minimum rigidity particles in primary cosmic ray spectrum, moves toward a higher rigidity as solar activity increases. Though this property was ascertained by observations at airplane altitudes (MEYER and SIMPSON, 1957), the report based on sea level measurements has been scarcely given up to now.

Finally, descriptions are given of several applications of the results deduced from the study of geomagnetic effects to other experimental results. Both the threshold rigidities and the response functions are the most fundamental characters necessary for studies of time variations of cosmic ray intensity. Typical examples of such applications are discussed.

The present report is a summary of the related articles published during 1961–66, with some revisions and more details.

PART 1. GEOMAGNETIC EFFECTS OF COSMIC RAY INTENSITY

1. 1. Introduction

As part of the Japanese Antarctic Research Expedition programs during 1956–1962, five latitude surveys for cosmic ray measurements were made on board the SOYA along a definite route as shown in Fig. 1. The period of each survey is indicated in Fig. 2, where we referred to the monthly averages of bihourly counting rate of the neutron monitor at Mt. Washington and the sunspot relative number. Each survey was stated in October or November every year and was finished in April or May of the next year, excepting 1957–1958. The data thereby obtained have been analyzed together with other neutron data from similar surveys as follows; LABRADOR and ATKA by ROSE *et al.* (1956), ARNEB by SIMPSON *et al.* (1963) and LEIPZIG by SKORKA (1956). The voyage routes and the observation periods of these surveys are indicated in Figs. 1 and 2, respectively. All of the cosmic ray surveys utilized in the present analysis are summarized in

Table 1. List of the sea-level latitude surveys from which cosmic ray data are analyzed.

Survey No.	Ship	Survey period	Counts/hour*	Standard error/day	Barometric coefficient
1	LABRADOR	Jul. 1954–Nov. 1954	10,000	0.20%	−0.735%/mb
2	ATKA	Dec. 1954–Apr. 1955	10,000	0.20	〃
3	ARNEB–I	Nov. 1955–Apr. 1956	10,000	0.20	〃
4	LEIPZIG	Sept. 1956–Jan. 1957	5,000	0.29	−0.74
5	ARNEB–II	Oct. 1956–Apr. 1957	10,000	0.20	−0.735
6	SOYA–I	Nov. 1956–Apr. 1957	8,000	0.23	−0.76
7	SOYA–II	Nov. 1958–Apr. 1959	7,000	0.24	〃
8	SOYA–III	Nov. 1959–Apr. 1960	12,000	0.18	〃
9	SOYA–IV	Nov. 1960–May 1961	12,000	0.18	〃
10	SOYA–V	Oct. 1961–Apr. 1962	7,000	0.24	〃

* Approximated value above the latitude knee.

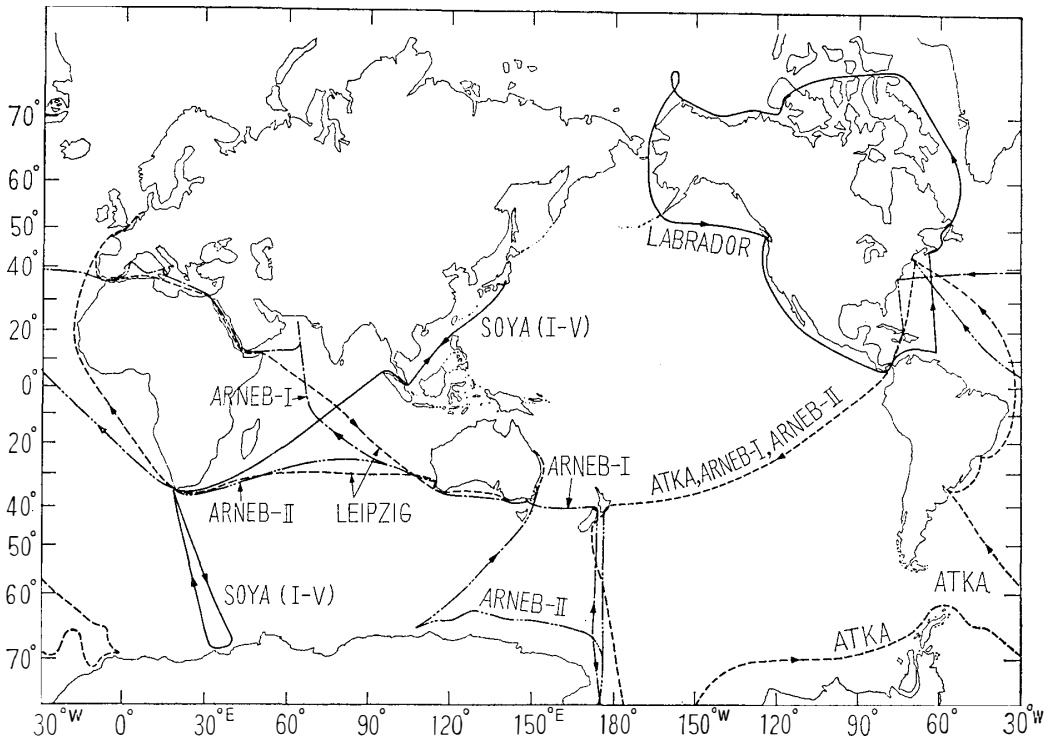

Fig. 1. Various ship routes along which cosmic ray measurements were carried out. The ship name is attached to each route.

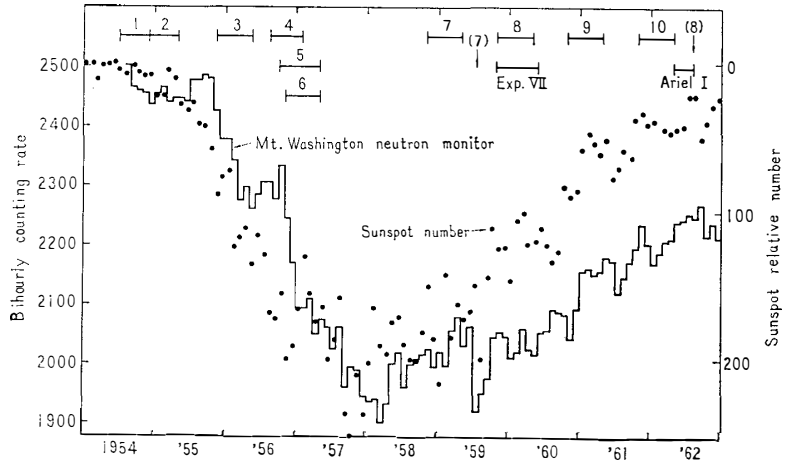

Fig. 2. Cosmic ray intensity variation recorded by Mt. Washington neutron monitor and Zürich relative sunspot number during 1954–1962. The periods of the shipborne and the satellite measurements are denoted by horizontal lines, where attached figures are designated in Table 1.

Table 1. In the case of the SOYA, differences among the counting rates are attributable to any one or two of changes in 1) the location of the observation room aboard, 2) shielding materials surrounding the observation room and 3) the electronic equipment.

It has already been demonstrated by several workers that the threshold rigidity determined from calculations of a series of trajectory traces of cosmic ray particles, assuming a proper geomagnetic field simulation, is superior to those obtained by analytical methods. For example, KELLOGG (1960) and SHEA *et al.* (1964) gave clear evidence with respect to the position of the cosmic ray equator, and KONDO *et al.* (1963) and KONDO and KODAMA (1965) with respect to the latitude effect in intensity. In addition, KODAMA (1965) and SHEA *et al.* (1965b) gave the threshold rigidities for a number of particular neutron monitor stations on the earth. In this work, the trajectory calculations have been performed for selected points along the ships routes given in Table 1, and extended further for a number of grid points selected in geographic coordinates in order to prepare a table giving the world-wide distribution of the vertical threshold rigidities.

There exists an intense anomaly of the horizontal magnetic intensity around Cape Town, the area which the SOYA passed through twice in a single voyage. Hence, the spatial distribution of cosmic ray intensity in that area would be of interest for the study of higher term effects of the geomagnetic field on cosmic ray intensity, particularly in reference to the position of the latitude knee.

1. 2. Reduction of data

All of the cosmic ray data obtained from the latitude surveys were converted into natural logarithms for representation of relative intensity. This logarithmic representation is convenient especially for a remarkable change as in latitude effect, when comparing the data obtained under different observational conditions with one another. After conversion, they were corrected for the atmospheric pressure and the world-wide short term variation such as FORBUSH decrease, where the meson component was corrected for the atmospheric pressure and temperature. Strictly speaking, the barometric coefficient for the nucleonic component varies with latitude and solar activity (for example, SIMPSON and FAGOT, 1953; GRIFFITHS *et al.*, 1966). However, a fixed value of the coefficient was applied to each survey, because the statistical accuracy in measurements is not so high (cf. Table 1).

In order to correct for world-wide variations, the latitude dependence of world-wide variations was determined using neutron data collected at 18 cosmic ray stations. After seven remarkable FORBUSH decreases that occurred during July–December 1957 were averaged in intensity, a latitude curve of a ratio α of the decrement observed at Mt. Norikura to that in any other latitudes was drawn as shown in Fig. 3. Thus, the world-wide correction was applied to the data from the SOYA voyages by reference to Mt. Norikura neutron intensity variation

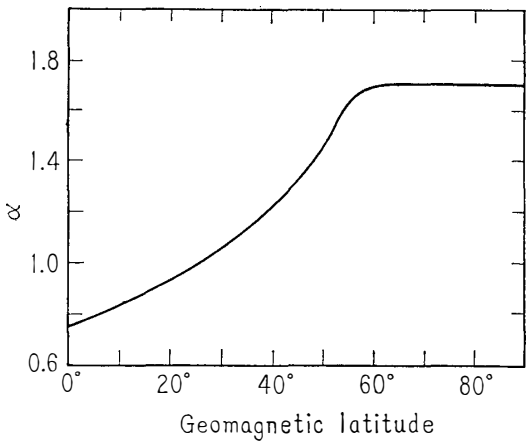

Fig. 3. Latitude dependence of the world-wide variation of cosmic ray neutron intensity when normalized to that in Mt. Norikura station.

multiplied by α.

On a process of barometric correction, there is a noticeable matter regarding the availability of pressure data. It is well known that a considerable amount of depression may be introduced occasionally in actual readings of barograph under a blow of high wind. Thus, readings of the conventional marine barograph aboard the ship at sea would be much more disturbed than at fixed stations. Though the statistical accuracy in individual cosmic ray measurement is as given in Table 1, it must be noted that systematic errors due to such pressure deviation may become large, occasionally surpassing the statistical one.

1. 3. Trajectory calculations of the threshold rigidities

The present calculations for determination of the threshold rigidities were carried out by a procedure similar to the computer program developed by McCRACKEN *et al.* (1962), using three kinds of computers*. The fundamental procedure for calculations is as follows.

The equation of motion of a charged particle in the magnetic field $\boldsymbol{B}$,

$$\frac{d^2\boldsymbol{r}}{dt^2}=\frac{e}{mc}\left(\frac{d\boldsymbol{r}}{dt}\times\boldsymbol{B}\right), \tag{1}$$

can be converted into terms of the spherical co-ordinate system as follows:

$$\left.\begin{aligned}
\frac{dv_r}{dt}&=\frac{e}{mc}(v_\theta B_\phi-v_\phi B_\theta)+\frac{v_\theta^2}{r}+\frac{v_\phi^2}{r}\\
\frac{dv_\theta}{dt}&=\frac{e}{mc}(v_\phi B_r-v_r B_\phi)-\frac{v_r v_\theta}{r}+\frac{v_\phi^2}{r\tan\theta}\\
\frac{dv_\phi}{dt}&=\frac{e}{mc}(v_r B_\theta-v_\theta B_r)-\frac{v_r v_\phi}{r}-\frac{v_\theta v_\phi}{r\tan\theta}\\
\frac{dr}{dt}&=v_r,\quad \frac{d\theta}{dt}=v_\theta,\quad \frac{d\theta}{dt}=\frac{v_\phi}{r\sin\theta},
\end{aligned}\right\} \tag{2}$$

where $\boldsymbol{r}$: position vector of a particle
r: radial distance from the center of the earth
θ: co-latitude

* IBM 7094, University of Chicago Computation Centre, U. S. A., Bendix G-20, Atomic Energy of Canada Limited, Canada, and OKITAC-5090H, the Institute of Physical and Chemical Research, Tokyo.

ϕ: longitude measured eastward from Greenwich meridian
v_r, v_θ, v_ϕ: velocity component in r, θ, ϕ directions.

This set of differential equations can be solved numerically if three components of the magnetic field, B_r, B_θ, B_ϕ are given. Now a magnetic potential U, which can be expanded in spherical harmonics, is defined as follows:

$$U(r,\theta,\phi)=a\sum_{n=1}^{\infty}\sum_{m=0}^{n}(g_n^m\cos m\phi+h_n^m\sin m\phi)\,P_n^m(\cos\theta)\left(\frac{a}{r}\right)^{n+1}, \qquad (3)$$

where g_n^m and h_n^m are the Gaussian coefficients, $P_n^m(\cos\theta)$ are the partially normalized Legendre functions and a is the average radius of the earth (CHAPMAN and BARTELS, 1951). The magnetic components at the point (r, θ, ϕ) is then represented by

$$B_r=-\frac{\partial U}{\partial r},\quad B_\theta=-\frac{1}{r}\frac{\partial U}{\partial\theta},\quad B_\phi=-\frac{1}{r\sin\theta}\frac{\partial U}{\partial\phi}. \qquad (4)$$

Since values of the coefficients g_n^m and h_n^m are given by several workers, $\boldsymbol{B}$ is known at all points by the eq. (4). It is, therefore, possible to determine the trajectory of a cosmic ray particle by numerical integration of the eq. (2). In practice, the GILL modification of the RUNGE-KUTTA integration process is used for a successive method in which the computed data at a point on the trajectory is utilized for the computation at a subsequent point on the trajectory (GILL, 1951).

In this work, the geomagnetic field simulation used in the eq. (3) was that of FINCH and LEATON (1957) except in special cases. The path of a negatively charged particle having a certain magnetic rigidity was traced outward in a vertical direction from an initial point at the top of the atmosphere (20 km above sea level). Computations were continued until its radial distance from the center of the earth became either greater than 25 earth radii (allowed orbit) or less than the earth radius (forbidden orbit), and were stopped when the total number of integrations for a trajectory reached 7,000 (incomplete orbit).

In general, the trajectories become complicated occasionally in middle latitudes because of the penumbral effect. The total number of the RUNGE-KUTTA-GILL integration steps necessary for determination of a trajectory varies widely from a few hundreds to several thousands, depending on the geographic coordinate of the starting point of the trajectory. For example, the cosmic ray particle having the rigidity of 5.1 GV can enter a point of 42.2°N, 9.7°W geographic after three rounds around the earth during which the integration steps of 5197 were employed. The threshold rigidity of a point can be determined from a sequence of the trajectory calculations repeated as a function of rigidity. SHEA *et al.* (1965a, b) adopted 0.01 GV as the rigidity interval. In our case, the calculations were performed at intervals of 0.1 GV. The threshold rigidities based on this interval seem to be suitable for analyses of the data obtained from the present cosmic ray measurements, of which accuracies were not so high statistically. Even if it is not suitable, some ambiguities will be inevitable in the procedure of calculations of the threshold rigidities, particularly in middle latitudes. As the origin of the errors included in the trajectory-computed threshold

rigidities, the following three could be considered.

1) The threshold rigidity at a given point will depend upon the primary spectrum if the point has some penumbra. Assuming $P^{-N}dP$ as a differential response function, the effective threshold rigidity, P_c, is calculated for different values of N using the equation,

$$\int_{P_c}^{\infty} P^{-N}\, dP = \int_{0}^{\infty} G(P)\, P^{-N}\, dP, \tag{5}$$

where $G(P)=1$ for non-reentrant trajectory, and $G(P)=0$ for 'incomplete' or 'reentrant' trajectory. The word 'incomplete' means that the trajectory is still trapped between 1 and 25 earth radii in the geomagnetic field. The word 'reentrant' means that the trajectory intersects the earth's surface when the integration stops. Now, since dP is finite, the eq. (5) is approximated by

$$\sum_{P_c'}^{\infty} P^{-N}\, \Delta P = \sum_{0}^{\infty} G(P)\, P^{-N}\, \Delta P. \tag{6}$$

In the present work $\Delta P=0.1$ GV and the value of $P_c=P_c'-0.05$ depends upon N. Since the response function for the sea-level nucleonic component can be approximated by $P^{+0.5\sim-0.5}$ in the rigidity range where the penumbral effect is important (WEBBER, 1962), zero will be a lower limit of N. While, $N=5$ will correspond to an extreme spectrum of solar proton events (for example, WINCKLER, 1962). As an example, the value of P_c at the geographic location of 20°S, 150°E is 11.05 GV and 10.42 GV for $N=0$ and $N=5$, respectively (KONDO, 1966).

Another source of the error is considered as follows. If a region between two adjacent rigidities spaced by 0.1 GV is completely either plus or minus 0.1 GV, and if the number of such similar regions is R, then the error would be

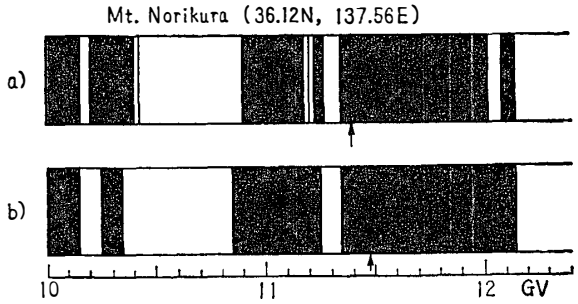

Fig. 4. Detailed illustrations of the penumbral bands for Mt. Norikura calculated on the basis of 0.01 GV integration steps by SHEA *et al. (upper) and 0.1 GV steps (lower). The forbidden trajectories are in black. Arrows show* P_c.

0.1 R GV. If the occurrence of R greater than 1 is improbable, it would be, in general, reasonable to estimate an error of ± 0.1 GV from this cause. Indeed, the value of P_c for Mt. Norikura station, of which the calculated penumbral bands are illustrated in Fig. 4, is 11.39 GV and 11.47 GV for calculations in 0.01 GV (SHEA *et al.*, 1965a) and 0.1 GV rigidity intervals, respectively. However, SHEA *et*

al. (1965b) showed an example that calculations by rigidity intervals of 0.01 GV give the deviation from 3.60 GV to 4.03 GV for the effective cutoff of 3.72 GV. Therefore, the above estimation of ± 0.1 GV may be a lower limit.

2) A trajectory for which the total number of the integration steps is more than 7,000 is defined as 'incomplete' in this work, but the numerical value, 7,000, is quite arbitrary, so some error might result from this arbitrary limitation. For example, if a particle starting from the earth's surface ultimately escapes beyond 25 earth radii only after say 10,000 iterative steps, then the effective threshold rigidity should be reduced by 0.1 GV. However, it is rather difficult to say that such a trajectory belongs to the allowed cone for the actual cosmic ray particles, because it will have had so many complicated rotations around the earth, possibly resulting in energy loss for the particles. It is, however, hard to estimate quantitatively the magnitude of the error based on this cause.

3) The threshold rigidity depends upon the model of the geomagnetic field simulation employed. The simulation should be influenced by the facts that the geographic distribution of the data from magnetic surveys is not always uniform over the world and also there is a secular variation in the magnetic field intensity. In Table 2 are given the threshold rigidities corresponding to the three

Table 2. Comparisons of the effective threshold rigidities calculated using the three different simulations of the geomagnetic field.

Station	(A) FINCH & LEATON*	(B) JENSEN & CAIN*	(C) CAIN *et al.*	(A)−(C)
Deep River	1.02	1.04	1.15	−0.13
Hermanus	4.90		4.64	0.26
Huancayo	13.49	13.36	13.35	0.14
Irkutsk	3.74		3.74	0.0
Kodaikanal	17.47		17.45	0.02
Mexico City	9.53		9.24	0.29
Mt. Norikura	11.39	11.46	11.05	0.34
Rio de Janeiro	11.73		11.65	0.08
Rome	6.31		6.14	0.27
Yakutsk	1.70		1.75	−0.05

* By SHEA *et al.* (1965b).

different simulations: one by FINCH and LEATON (epoch–1955, British Admiralty Charts), another by JENSEN and CAIN and still another by CAIN *et al.* (epoch–1960, U. S. Hydrographic Office Charts). The differences among the threshold rigidities based on these three simulations are not negligibly small, mainly due to the fact that the CAIN *et al.*'s dipole term is about 0.4% lower than that of FINCH and LEATON. The r. m. s. deviation of the differences between the simulation by FINCH and LEATON and that by CAIN *et al.* is about 0.2 GV, being 2.5% of

the rigidity value averaged over the ten cosmic ray stations as listed in Table 2. It is noticeable that the difference is significantly dependent upon the geographical location. This fact would be of importance particularly for a plot of cosmic ray intensity as a function of threshold rigidity.

Table 3. The number of the points where the trajectory calculations were made.

Ship	LABRADOR	ATKA	ARNEB-I	LEIPZIG	ARNEB-II	SOYA	Total
Number	23	47	34	53	27	48	232

The present trajectory calculations were performed for a number of specific points along the cosmic ray survey routes as shown in Fig. 1. The number of the calculation points actually selected is summarized in Table 3. In addition, the calculations were extended to 125 grid points in geographic co-ordinates in order to prepare the world-wide distribution of the vertical threshold rigidities. Results of the former will be described in the next section and those of the latter in section 1.9. Furthermore, some subsidiary calculations were made to examine the influence of both the geomagnetic field simulation and the incoming directions of cosmic ray particles upon the vertical threshold rigidity.

1.4. Latitude variation of the cosmic ray intensity

For the purpose of demonstrating the geomagnetic effects on cosmic ray intensity, it is convenient generally to plot the observed intensity as a function of the threshold rigidity. Then, the scattering of each plotted point from a single intensity-rigidity curve gives a good measure to check the reliability of both physical quantities. In the following subsections 1.4.1 to 1.4.5, daily or semi-daily mean values of the cosmic ray intensities obtained from the surveys of Table 1 will be compared critically with each of both the trajectory-computed threshold rigidities (hereafter denoted by T-value) and the QUENBY and WENK's threshold rigidities (QW-value), which hitherto have given the best approximation among the different sets of values obtained analytically. The QW-values were determined from a linear interpolation of their numerical table for corresponding ship positions.

1.4.1. SOYA survey

Since the ship route is almost the same in the voyages both outward and homeward, a set of the intensity-rigidity curve can be deduced in the geographical latitude range from 35°N to 69°S. In Fig. 5 is illustrated an example of the neutron intensity *versus* the threshold rigidity in the last survey of 1961–62. Double circles are the rigidity values determined from the exact trajectory calculations, while black ones are those extrapolated from the QW-values. Also, points involving the penumbral effects are denoted with *P*. It can be clearly seen that an application of the T-value considerably improves the shape of the

QW-rigidity curve in the southern hemisphere, as indicated by arrows. In Fig. 6, the survey regions where such a remarkable improvement is found are sketched roughly in its degree, in order to see a possible connection between the regions and the worldwide distribution of the horizontal magnetic intensity (U. S. Navy Hydrographic Office, epoch 1955).

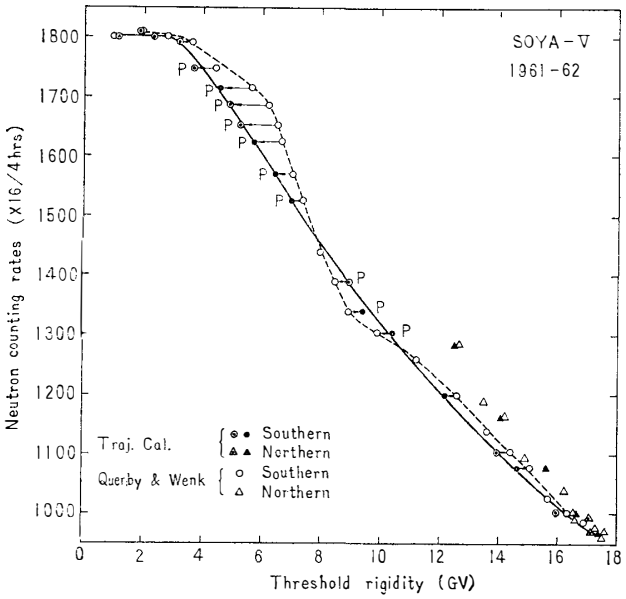

Fig. 5. Neutron intensities from the 1961–62 SOYA voyage are plotted as a function of each of the trajectory-computed threshold rigidities and the QUENBY and WENK's values. Double circles denote the rigidity values determined from the exact trajectory calculations, and black ones those extrapolated from the QUENBY and WENK's values. Also, points involving the penumbral effects are indicated by P.

Now, let us discuss about the data obtained in the northern hemisphere which are indicated by triangle marks in Fig. 5. If the disagreement of the data between the two hemispheres is reliable, then the following could be considered as the possible origins of this discrepancy: 1) effect of the cosmic ray particles arriving from inclined directions, 2) FINCH and LEATON expression adopted here may not be good enough to represent the real geomagnetic field, and 3) time variations in neutron intensity. In order to examine the first, the trajectory calculations for cosmic ray particles inclined by 30° from the zenith were performed for two locations between which the largest northern-southern intensity difference, about 4%, was found. The results computed are summarized in Table 4, where ΔI means the amount of intensity change deduced from ΔP assuming $\cos^6\theta$ as the zenith angle dependence for the nucleonic component. Table 4 suggests that half of 4% may be explained by the effect of inclined particles.

Ragarding the second, we have now several simulations, besides the FINCH and LEATON simulation, for representing the geomagnetic field. Using one of them, JENSEN and WHITAKER (1960), the same calculations were tried for comparison with the FINCH and LEATON simulation. The numerical results, as also seen in Table 4, have the correct sign to explain the above discrepancy, but the amount is too small.

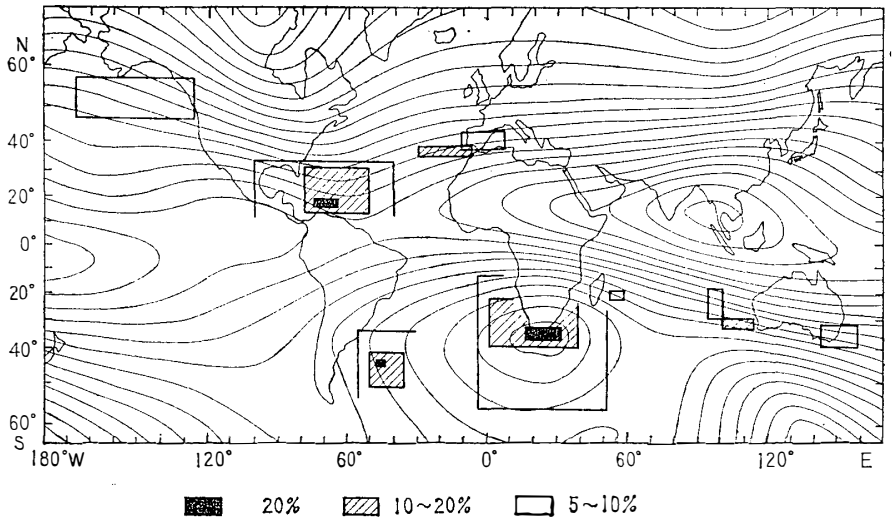

Fig. 6. World-wide distribution of the difference between the trajectory-computed threshold rigidities and the QUENBY *and* WENK*'s values is shown by rectilinear area in their degree. Contour lines give the horizontal magnetic intensity.*

Table 4. Threshold rigidities for inclined cosmic ray particles and for JENSEN *and* WHITAKER *simulation.*

Location		Threshold rigidities P in GV					
Geogr. lat.	Geogr. long.	Vertical	30°N	30°E	30°S	30°W	JENSEN & WHITAKER
34.5	139.0	12.65	10.95	17.35	11.85	9.75	12.35
−15.3	65.9	12.55	12.45	18.15	13.65	9.90	12.45
ΔP (%)		+0.8	−12.8	−4.5	−14.2	−1.5	−0.8
ΔI (%)		+0.5	− 3.0	−1.0	− 3.6	−0.4	−0.5

Last, the magnitude of the northern-southern difference varies a little with time, but less often. According to the recent survey aboard the FUJI, which has been carried out with better statistical accuracy during 1966–67, such intensity difference was scarcely recognized (KODAMA and OHUCHI, 1968). But even if the long-term variation of the northern-southern difference is significant, its cause is open to question.

Now, daily averages of the pressure corrected meson intensities obtained from the three surveys, 1956–57, 1960–61 and 1961–62, are plotted against the threshold rigidities in Fig. 7, where open and black circles denote the QW-value and the T-value, respectively. The discrepancy in intensity-rigidity curve between the northern and southern hemispheres was found in the first and last surveys, as in the case of the nucleonic component. Fractional changes of the latitude factors of the nucleonic and meson components are given in Table 5 together with the

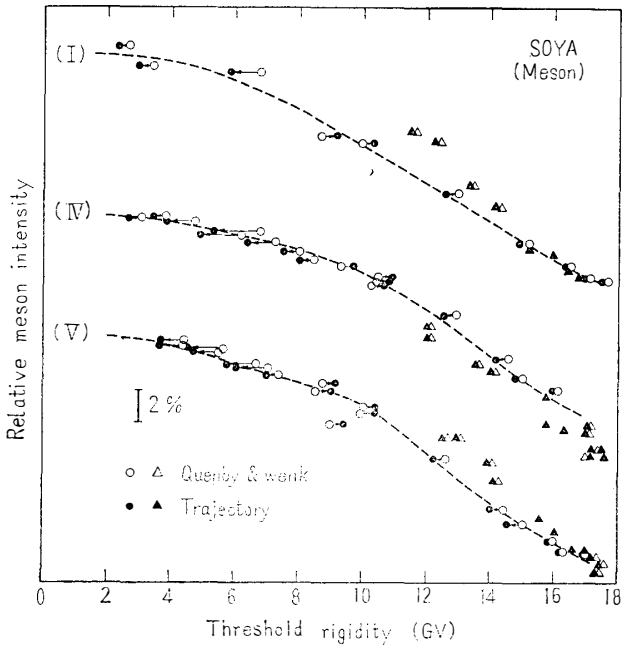

Fig. 7. Meson intensities from the SOYA voyages, 1956–57, 1960–61 and 1961–62, are plotted as functions of trajectory-computed threshold rigidities and the QUENBY and WENK's values.

ratio between them. The maximum intensity level above the latitude knee was obtained from the average intensiy for about two months staying of the ship in the Antarctic Ocean. When the atmospheric temperature correction was applied to the meson intensity, approximately using the sea-level temperature data, its latitude factor and the ratio are given in brackets of Table 5.

Table 5. Fractional latitude factor of cosmic ray neutron and meson components in % and its ratio between them.

Survey No.	6	7	8	9	10
Neutron	64.1	56.9	55.7	58.9	62.0
Meson	16.7(13.0)	—	—	17.5(13.8)	18.7(15.0)
N/M ratio	3.84(4.92)	—	—	3.36(4.27)	3.32(4.13)

A correlation diagram between the meson and neutron intensities as a function of geographic latitudes is given in Fig. 8, where the meson intensity was multiplied by the ratio listed in Table 5 to normalize the amount of the latitude variation. It can be seen that the experimental points in each survey do not always reveal a similar pattern of latitude variation for both components over the entire latitude range but deviate systematically downward from a 45° inclined line in the latitude range 25°S to 50°S geographic. No evidence of a considerable change of the room temperature was found in this latitude range. Thus, such a deviation would be attributable either to the atmospheric temperature effect of the meson component, or to a possible different fashion of influence of

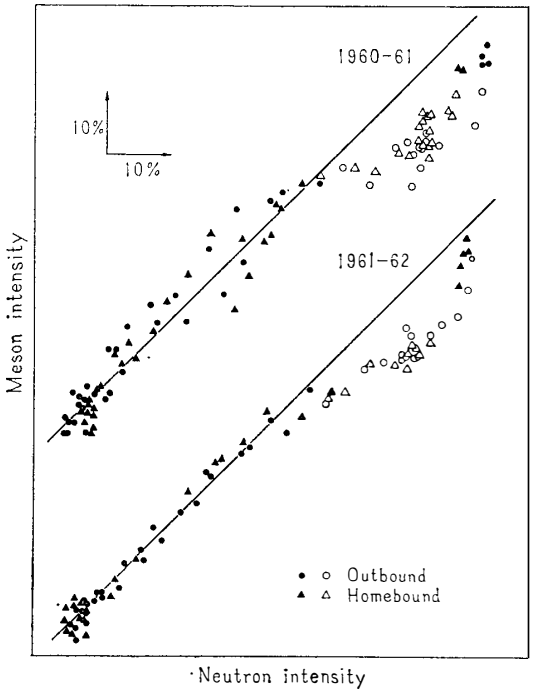

Fig. 8. Correlation between neutron and meson intensities from the SOYA voyages, 1960–61 and 1961–62, as a function of geographic latitude. Meson intensities are multiplied by 3.36 and 3.32 for 1960–61 and 1961–62 surveys, respectively. Open marks are used for data points belonging to the geographic latitudes 25°S to 50°S.

the Cape Town geomagnetic anomaly to both components. Further experiments with better accuracy will be desired, particularly for the meson component.

1. 4. 2. LABRADOR survey

The voyage started from Halifax in July 1954, going north through the North West Passage, and south along the Pacific Coast of North America, through the Panama Canal, then east to the Island of Grenada, and back to Halifax in November, 1954 (cf. Fig. 1). Two sets of latitude variations obtained from such circumnavigation of the North American continent are shown in Fig. 9, where twelve-hour averages were taken. Circles are used for the Pacific coast survey and triangles for the Atlantic coast survey, respectively. The geographical region where an appreciable improvement from the QW-value to the T-value was recognized is illustrated in Fig. 6. Also, the difference in the QW-value between

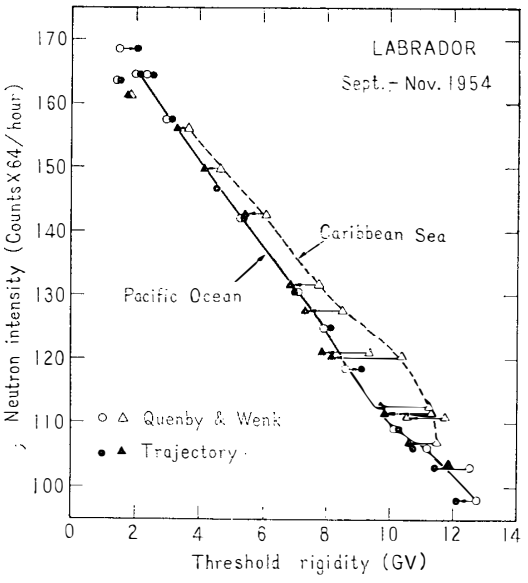

Fig. 9. Neutron intensities from the LABRADOR voyage versus trajectory-computed threshold rigidities and the QUENBY and WENK's values.

any two points giving the same level of cosmic ray intensity varies widely over two oceans, amounting to about 2 GV, while it is reduced to order of 0.5 GV for use of the T-value except a region near 8 GV. This discrepancy between the two different longitudinal regions, *i. e.*, between the Caribbean Sea and the North Pacific Coast, also will be proved by measurements aboard the ATKA and the ARNEB which crossed the Caribbean Sea on their voyages.

1. 4. 3. ATKA survey

The voyage started from Boston in December, 1954, and headed directly to the Panama Canal, then to New Zealand, south to the Antarctic, east around the coast of Antarctica, northwest to Buenos Aires and Rio de Janeiro, and back to Boston in April, 1955 (cf. Fig. 1). Figs. 10 and 11 show the latitude variations in the outbound and homebound voyages, respectively, where twelve-hour averages were used. In both cases, remarkably improved regions with respect to the threshold rigidity are indicated by rectangular area in Fig. 6. The rigidity difference, as appeared in Fig. 9, in the T-value between the different longitudes was observed again in a definite region around 8 GV, especially amounting to 1.4 GV between a point A (15.3°N, 76.5°W) in the Caribbean Sea and B (34.5°S, 144.0°W) in the South Pacific Ocean. Except these areas, the observed neutron intensities could be ordered with a good linearity as a function of the T-values.

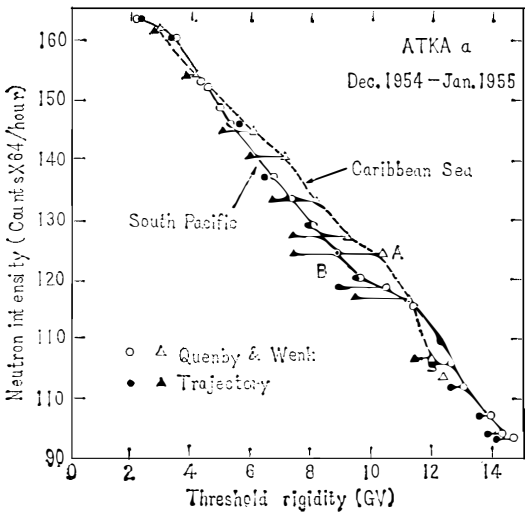

Fig. 10. Neutron intensities from the outbound voyage of the ATKA versus trajectory-computed threshold rigidities and the QUENBY and WENK's values.

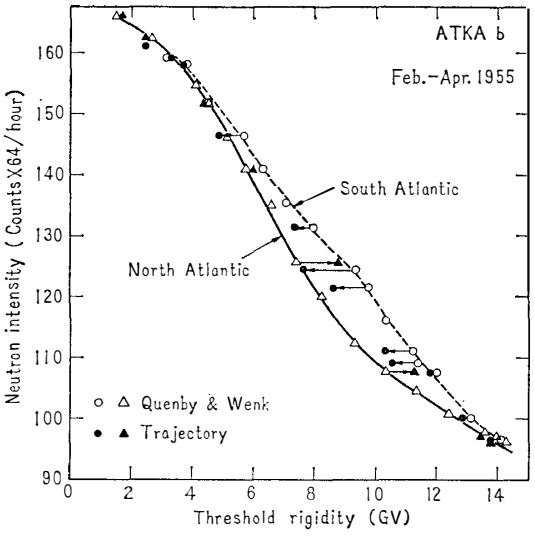

Fig. 11. Neutron intensities from the homebound voyage of the ATKA versus trajectory-computed threshold rigidities and the QUENBY and WENK's values.

1. 4. 4. ARNEB survey

The round-the-world survey was carried out twice during the period from

November 1955 to May 1957 (KONDO, 1966). The routes of the outbound voyages of both surveys to the Antarctica were almost the same with that of the ATKA, but their homebound voyage routes were somewhat different from each other. Namely, the first one (ARNEB–I) went north to New Zealand, then west to Australia, and back to New York through the Suez Canal, while the second (ARNEB-II) was across the Indian and Atlantic Oceans via Sydney and Cape Town (cf. Fig. 1). In the ARNEB–I survey, a comparison between two sets of latitude variations corresponding to different longitudinal regions is possible in the following two ways: one is made between the Caribbean Sea and the South Pacific Ocean, and another between the North Atlantic and Indian Oceans. Also, two sets of similar comparisons can be made in the ARNEB–II survey, where one of them is between the North and South Atlantic Oceans.

1. 4. 5. LEIPZIG survey

The voyage started from Rotterdam in August 1956, headed for the Suez Canal, then to Australia, and back to Bremen in January 1957 via Cape Town (cf. Fig. 1). In Fig. 12, the observed neutron intensities *versus* the threshold rigidities in the northern hemisphere are compared with those in the southern hemisphere. This diagram, too, proves that the T-value is much superior to the QW-value. In this case there is no appreciable discrepancy among different longitudinal areas when the T-values are used.

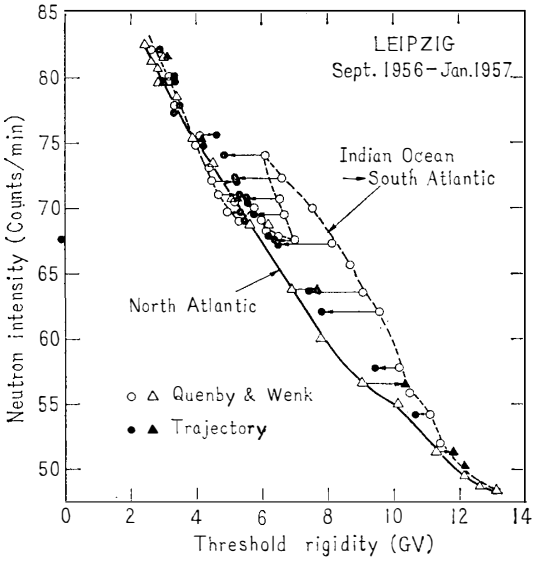

Fig. 12. Neutron intensities from the LEIPZIG voyage versus trajectory-computed threshold rigidities and the QUENBY and WENK's values.

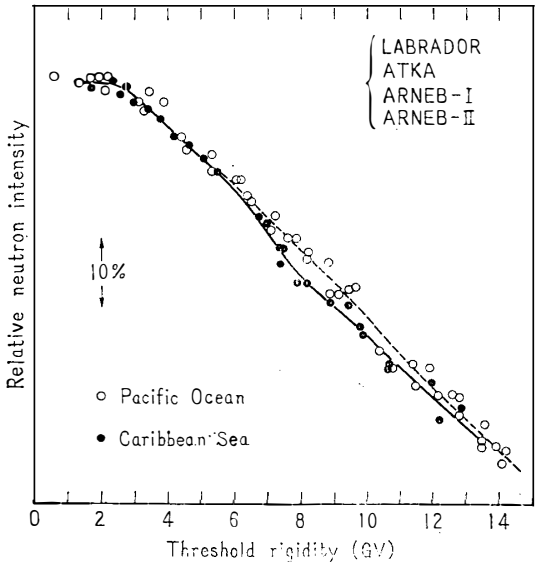

Fig. 13. A comparison of neutron intensities versus trajectory-computed threshold rigidities between the Pacific Ocean and the Caribbean Sea. The neutron data from LABRADOR, ATKA and ARNEB voyages are normalized with one another at the average level above the latitude knee.

In order to show quantitatively the degree of improvement from the QW-value to the T-value, the maximum and r. m. s. differences between both rigiditiy values were deduced for some selected points in each of the above surveys 1. 4. 1. –1. 4. 5. Results are shown in Table 6, where the differences are defined by [(T-value)–(QW-value)]/(T-value). Consequently, it is concluded from Table 6 that the r. m. s. difference between the T-value and the QW-value is 6.8% on an average.

Table 6. The maximum and the r. m. s. differences between the QUENBY and WENK's threshold rigidities and the trajectory-computed values.

Ship	Number of selected points	Maximum difference	RMS deviation of differences
SOYA	32	30%	14. 3%
LABRADOR	23	18	6. 9
ATKA–a	26	25	8. 1
ATKA–b	21	22	5. 6
ARNEB–Ia	14	25	8. 0
ARNEB–Ib	20	14	4. 0
ARNEB–IIa*	14	23	5. 8
ARNEB–IIb	27	33	8. 5
LEIPZIG	53	26	5. 9
Average		23. 9	6. 80

* Extrapolated values from the QW-values were assumed to the T-values.

In regard to the actual survey region, each of LABRADOR, ATKA and ARNEB crossed both the Caribbean Sea and the Pacific Ocean during their voyages. Also, the surveys in the North and South Atlantic Oceans were performed by ATKA, LEIPZIG and ARNEB–II. Accordingly, results obtained from these different surveys could be compared with one another, after normalizing the respective neutron intensities above the latitude knee. The former comparison is shown in Fig. 13, where open and black circles are used for the Pacific Ocean and Caribbean Sea surveys, respectively. It can be seen that a dashed line fitted to open circles is significantly apart from a solid line for black circles at the rigidity interval of about 7–10 GV. This discrepancy may be possibly due to the uncertainty of the FINCH and LEATON simulation adopted, because both survey regions seem to be affected by the Brazilian anomaly of the geomagnetic field.

A diagram for another comparison between the North and South Atlantic Oceans is given in Fig. 14, where open circles are used for the North Atlantic Ocean and solid ones for the South Atlantic Ocean, respectively. Though a small discrepancy between the two kinds of circles was found around 8 GV, their rigidity dependences as a whole coincide with each other. It may be, however,

noticeable that a few points included in a region of 6–7 GV deviate systematically from an overall latitude curve. Further discussion on this point will be given in section 1.7.

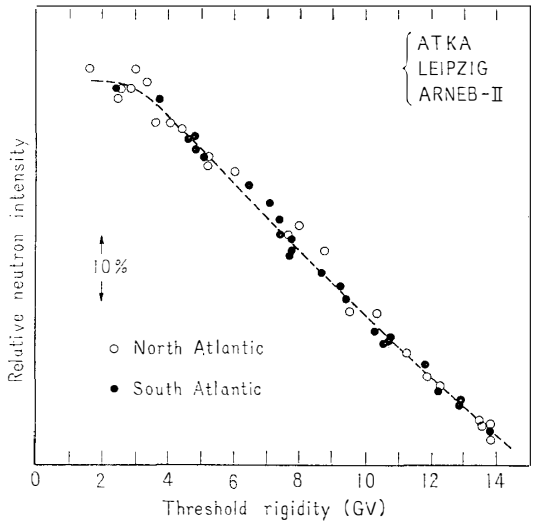

Fig. 14. Comparison of neutron intensities versus trajectory-computed threshold rigidities between the North and South Atlantic Oceans. The neutron data from ATKA, LEIPZIG and ARNEB-II voyages are normalized with one another at the average level above the latitude knee.

1.5. Cosmic ray equator

The routes of the ship mentioned above crossed the equator several times, where the minimum of the cosmic ray intensity was recorded along a specific geographic longitude. A line connecting the locus of these minimum intensity

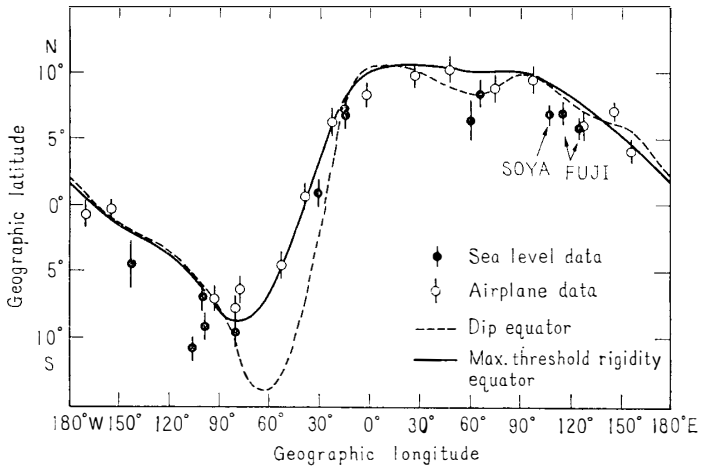

Fig. 15. Comparisons of the cosmic ray equator derived from trajectory calculations with experimental observations and the dip equator. The positions determined by the SOYA and FUJI surveys are designated.

points gives the so-called cosmic ray equator. Numerous studies have shown that the cosmic ray equator does not coincide with the geomagnetic equator, but that it is in good agreement with the equator as computed theoretically taking into account the non-dipole terms of the geomagnetic field (QUENBY and WEBBER, 1959; KELLOGG and SCHWARTZ, 1959; KELLOGG, 1960). The geographic latitude of the minimum intensity points was determined for the present surveys, and plotted as a function of the geographic longitude in Fig. 15, including other related experimental data. The equator point on the SOYA route, $6.7°N \pm 0.4°$, is given by a mean value of the results obtained from her five surveys. Also the locus of the maximum vertical threshold rigidities presently calculated* was traced on the figure, together with the dip equator. A fairly good agreement was found between the experimental points and the trajectory-computed equator.

Strictly speaking, most of the experimental points given by the airborne surveys lie near the computed equator, while those by the shipborne surveys deviate systematically to somewhat south from it. Two points recently obtained by KODAMA and INOUE (1968) aboard the FUJI in the Pacific Ocean and the South China Sea support such a southward deviation, as seen in Fig. 15. Based on the results of measurements of the geomagnetic field, OGUTI and KODAMA (1959) suggested that the difference between the dip equator and the cosmic-ray equator in 110°E geographic may be attributed to the former's incorrect position. Even when the results of the SOYA and the FUJI voyages were added, a significant difference between the experimental points and the computed equator is established in the geographic longitudinal region 110°–130°E. Thus, direct and repeated measurements of the geomagnetic field will be desirable in this area.

CHERNOSKY *et al.* (1964) pointed out that the locus of points, where the orientation of the magnetic field lines is referred to the mean noon altitude of the sun at equinox rather than to the earth's surface as is ordinarily done, coincides well with the dip equator and also KATZ *et al.*'s (1958) aircraft cosmic-ray equator. If such a seasonal change in the angle between the magnetic lines and incoming directions of cosmic ray particles can cause a possible latitudinal shift of the cosmic-ray equator, then the season when the cosmic ray measurement was made would be of importance. In the case of the SOYA surveys, all of the outward measurements were made before the December solstice and the homeward ones were after the spring equinox. Consequently, the cosmic ray minimum obtained from the outward voyage should be somewhat lower in latitude than that for the homeward voyage if such a seasonal effect is acceptable. Indeed, the average position of the observed equator was found to be $6.4°N \pm 0.1°$ and $6.9°N \pm 0.4°$ for the outward and homeward voyages, respectively (cf. Table 9 in page 37). Hence, the experimental results do not contradict, on an average, with this expectation, but the statistical significance of the difference in latitude between the two cosmic ray minima is not good enough. Even if the latter one, 6.9°N, is accepted as the true position, it is found to be located at 2.1° south of the theoretically com-

* Interpolated from Table 7.

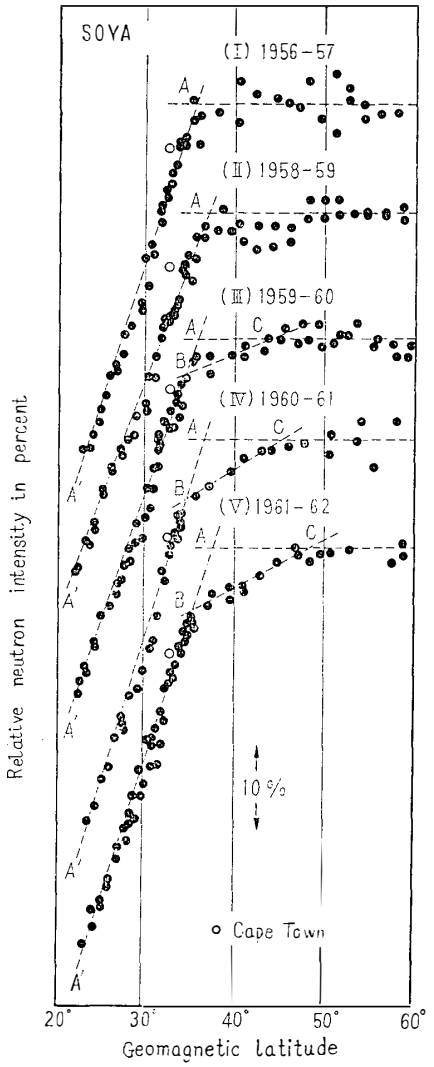

Fig. 16. Neutron intensities from five surveys of the SOYA versus the ordinary geomagnetic latitude. The intensity scale is given by the natural logarithmic representation of counting rates/12-hr (24-hr mean values for the forth survey only). The intensity shown by a horizontal line is deduced from the measurement during about two months when the ship was staying in the Antarctic Ocean.

puted equator. According to STOREY's (1959) airborne measurements at 145°E, the cosmic ray intensity minimum was at about 2.5° north of the computed equator. This position would be expected since the measurements were made in July near the June solstice. On the other hand, one of the FUJI minima was found at 5.8°N, 126.1°E in December 1967, being about 1.7° south of the computed equator. This may be expectable from the assumption of the seasonal change. However, since another one, 7.0°N, 115.0°E, was observed in April near the equinox, the difference of 1.5° south from the computed equator is inexplicable.

1. 6. Cosmic ray latitude knee around Cape Town anomaly

As mentioned in the preceding sections, an intense geomagnetic anomaly existing around Cape Town seriously affected the cosmic ray measurements by the SOYA. The apparent position of the so-called cosmic ray latitude knee, at about 35°S geomagnetic latitude, is found at much lower latitude than in other regions (KODAMA, 1960). Fig. 16 illustrates neutron intensities obtained from five surveys referring to the ordinary geomagnetic latitude based on the dipole field. If one defines the position of the knee as an intersection point of an inclined straight line fitted to observed points between 20°S and 35°S on the intensity-latitude curve with a horizontal line representing the mean neutron intensity level above 50°S, then it is clear from Fig. 16 that the position of the knee denoted by A scarcely shows systematic variations, of which error in latitude is estimated within $\pm 1°$. Whereas, we could find some difference in the apparent shape of the knee, varying from a sharp type to a gradual one with time. In other words, a difference between the neutron intensity at 35°S and that above 50°S becomes larger as

solar activity descends. On the other hand, the neutron component observed at a fixed cosmic ray station located near 35°S, Hermanus, shows intensity increase by 7.5 per cent during January 1958–March 1962, while 9.9 per cent at Mawson, Antarctica. Thus, such year-to-year variation in the latitude effect as seen in Fig. 16 is consistent with the observed results at the reference stations.

To display clearly the foregoing variation in the latitude effect, a straight line was approximately fitted with the points largely deviating from both the previous inclined and horizotal lines. When two intersection points of the present line with the previous ones are denoted by B and C, respectively, point B, the first knee, is always kept in a fixed latitude throughout the whole surveys, while point C, the second one, gradually moves towards higher latitude with time (KODAMA, 1963). However, when neutron intensities are plotted against the trajectory-computed threshold rigidities, the first knee disappears and a systematic year-to-year change is found in the position of the knee of the rigidity spectrum, as seen in Fig. 17. Recently, the corrected geomagnetic coordinates were presented by HAKURA (1965), taking into account the higher order terms of the geo-

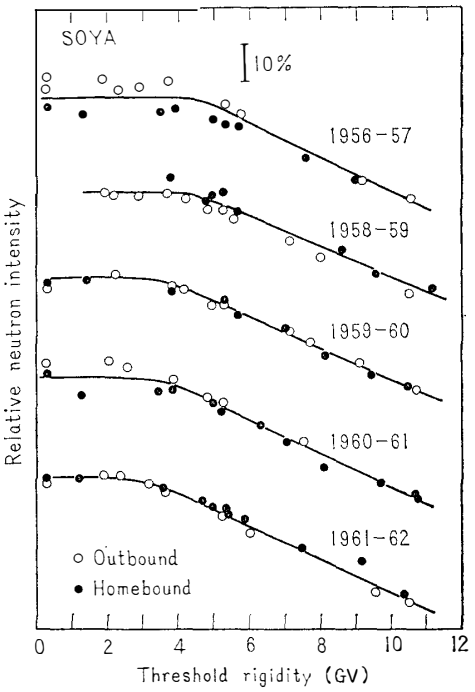

Fig. 17. Neutron intensities from five voyages of the SOYA versus the trajectory-computed threshold rigidities.

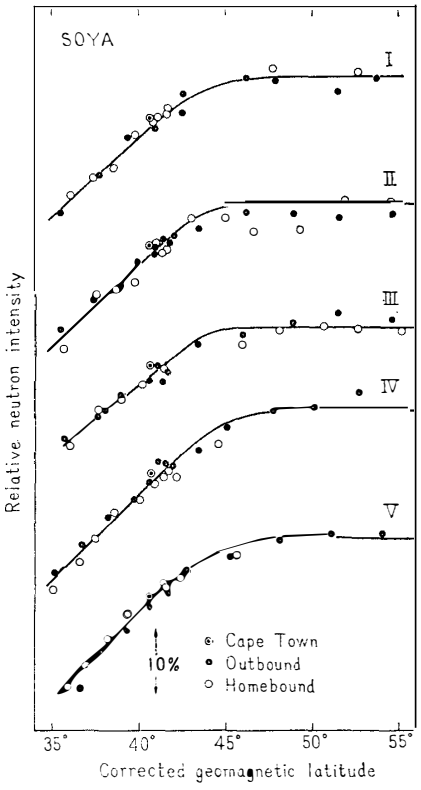

Fig. 18. Neutron intensities from five voyages of the SOYA versus the corrected geomagnetic latitude presented by HAKURA (1965).

magnetic field. When neutron intensities were plotted as a function of this corrected geomagnetic latitude as seen in Fig. 18, a single curve could be fitted to all points of outward and homeward voyages. In each case, the first knee as seen in Fig. 16 is not apparent and the second one alone remains. These facts suggest that the first knee is observable at sea level due to the influence of the geomagnetic anomaly around Cape Town, while the second one displays the inherent knee varying with the long term variation of the primary cosmic ray spectrum.

According to the latitude survey using an airborne neutron monitor performed around Cape Town by du PLOOY *et al.* (1963) in March 1962, the intensity-latitude curve arong 18.6°E geographic showed no 'knee' effect below 40.5°S in the ordinary geomagnetic latitude, which corresponds to 3.3 GV*. Since the position of the sea-level latitude knee in the last survey of the SOYA is found in 3 GV or smaller as seen in Fig. 17, no serious inconsistency exists between the sea-level knee and the high altitude knee (at 640 g/cm^2). Thus, the apparent position of the latitude knee referred to the ordinary geomagnetic latitude must be carefully dealt with, particularly in the case of the sea-level measurement sensitive to the geomagnetic anomaly which diminishes rapidly with height.

1. 7. Spatial distribution of the vertical threshold rigidities

For the study of the geomagnetic effects on cosmic rays it is convenient and useful to prepare a numerical table of the geographic distribution of the threshold rigidities, from which the threshold rigidity at any point on the earth can be interpolated easily. Although it is ideal to calculate the threshold rigidities corresponding to any incoming directions of cosmic ray particles, the utilization

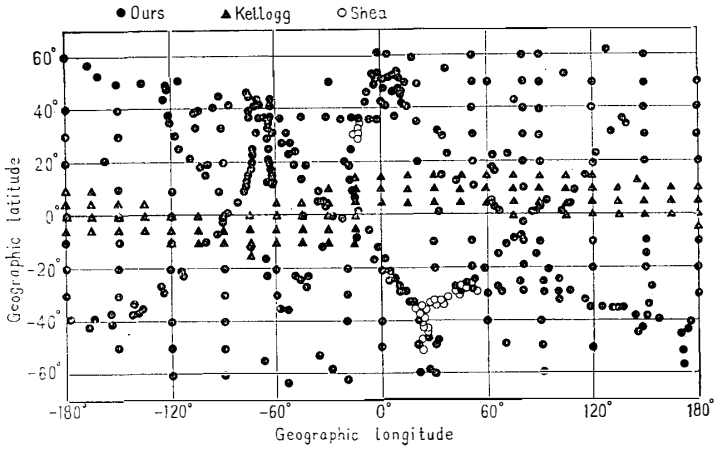

Fig. 19. World map showing the points at which the vertical threshold rigidities were determined from trajectory calculations.

* Computed using Table 7.

of the vertical threshold rigidity would be satisfactory at the present stage if one takes into account the tremendous amounts of calculations involved and the limitation of the present experimental accuracy. For this purpose, trajectory calculations were extended for 125 grid points in geographic coordinates, and the computed results for 208 points by KELLOGG (1965) and SHEA (1965) were utilized. Combining the results from all calculation points including 232 points already calculated for the sea-level surveys, a table of the vertical threshold rigidities at 5° latitude and 10° longitude intervals was prepared as shown in Table 7. The position of the calculation points adopted is indicated in Fig. 19. For convenience, contours of equal vertical threshold rigidities are drawn on a Cartesian and the polar geographic coordinates in Fig. 20 and Fig. 21. The practical procedure for preparation of Table 7 is described below.

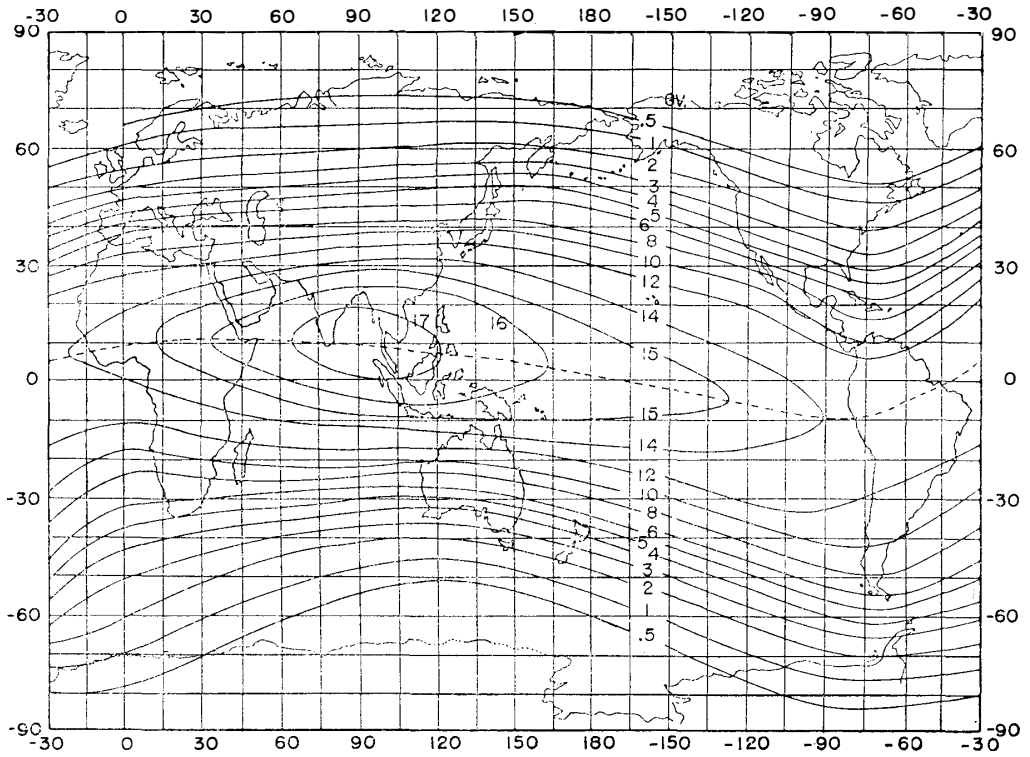

Fig. 20. Contour map of the vertical threshold rigidities, determined by the trajectory tracing method, plotted using Cartesian geographic coordinates.

In the first stage, a tentative table of 5° latitude and 10° longitude mesh was made, by interpolation, using original data at all the trajectory computed points. Next, values corresponding to the original points were computed using the tentative table, and then compared with the original values. After the first table was corrected for the difference between the original and the interpolated values, new values at original points were computed again using the second corrected table. This progressive method was repeated until the above difference

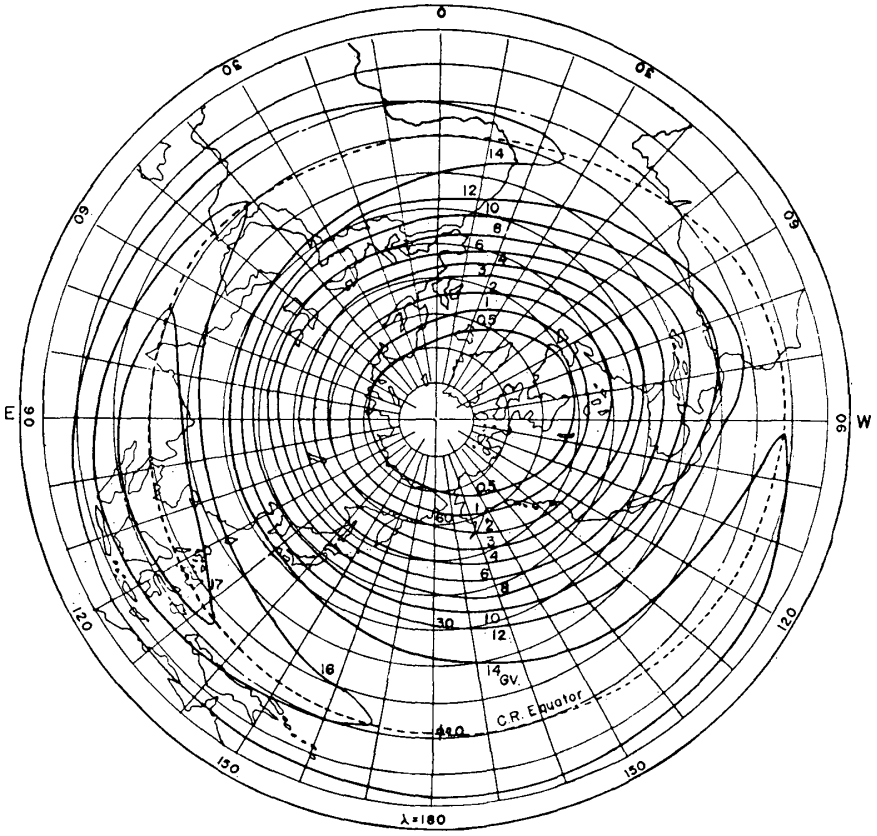

Northern hemisphere

Fig. 21a. Contour map of the vertical threshold rigidities, determined by the trajectory tracing method, plotted using polar geographic coordinates.

became well below the limitation of mathematical confidence.

In high latitudes where the threshold rigidity is less than 1 GV, the trajectory calculation is not only very laborious but also cannot be performed efficiently. Then the following method was proved to be sufficient for the determination of the threshold rigidity. The Störmer cone rigidity P_s at geomagnetic latitude ϕ in the dipole field is expressed by

$$P_s = P_d \cos^4 \phi, \tag{7}$$

where $P_d = 14.89$ GV. At the same time, the equatorial distance R_o (in unit of earth radius) of the magnetic line of force originating from the same point is expressed by

$$R_o = 1/\cos^2\phi. \tag{8}$$

Then P_s and R_o are related by

$$P_s = P_d/R_o^2. \tag{9}$$

In the geomagnetic field including the higher order terms, it is necessary to

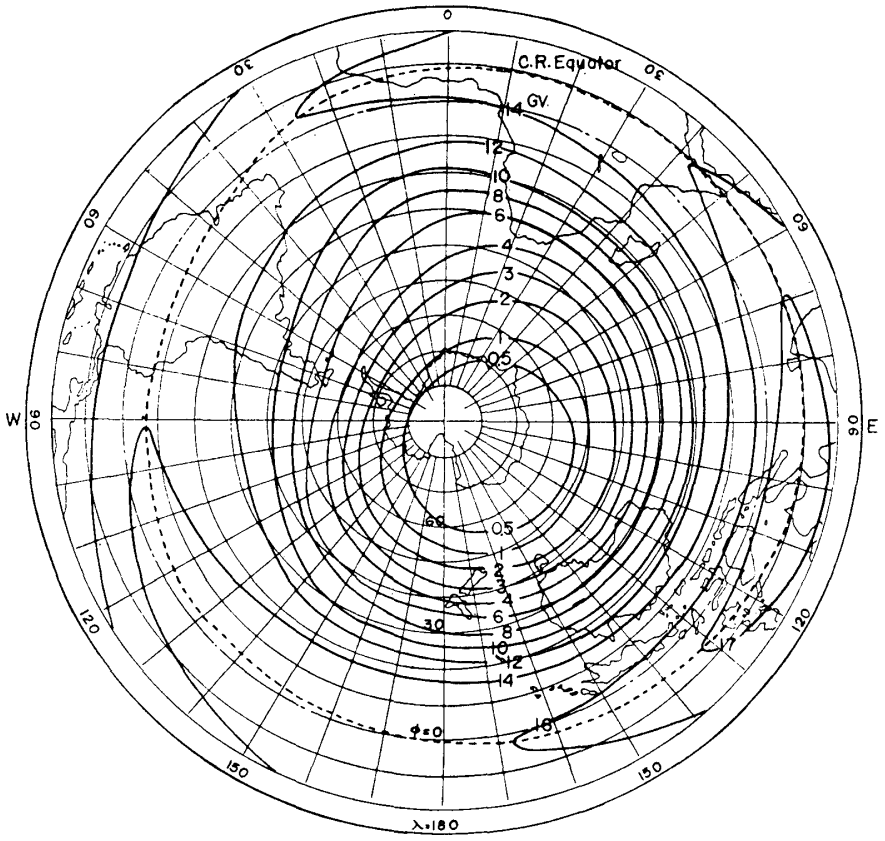

Fig. 21b. Contour map of the vertical threshold rigidities, determined by the trajectory tracing method, plotted using polar geographic coordinates.

find a quantity equivalent to R_o in the dipole field. If one traces a magnetic line of force from a point on the earth using the higher order simulation of the geomagnetic field and finds the minimum total magnetic field intensity B_o on the line of force,

$$L_o = \frac{(M/B_o)^{1/3}}{R_e} \quad (R_e = 6371.2\text{km}) \qquad (10)$$

is found to be equivalent to R_o (STONE, 1963), where M is the dipole moment of the earth (8.06×10^{25} gauss cm^3). Then one can use $P_l = P_d/L_o^2$ as an estimate of the Störmer cone rigidity. Actually it was found that the threshold rigidities less than 1.5 GV were almost the same with P_l. HAKURA (1965) applied this fact to the analysis of PCA events, where a radial distance R_o of the minimum field intensity point was used instead of L_o. Since the practical integration of the magnetic line of force is much easier than that of the trajectory, P_l was used to check the results of the trajectory calculations even in lower latitudes.

Last, some amendment was applied to the region where the spatial distribu-

Table 7. Vertical threshold rigidities determined from trajectory calculations (in GV).

Geogr. lat.	Gegraphic longitude																																		Geogr. lat.
	10	20	30	40	50	60	70	80	90	100	110	120	130	140	150	160	170	180	−170	−160	−150	−140	−130	−120	−110	−100	−90	−80	−70	−60	−50	−40	−30	−20	−10	0	
85	.01	.02	.02	.02	.03	.03	.03	.03	.04	.04	.04	.04	.03	.03	.03	.03	.02	.02	.02	.01	.01	.00	.00	.00	.00	.00	.00	.00	.00	.00	.00	.00	.00	.00	.01	.01	85
80	.04	.06	.07	.08	.09	.09	.10	.11	.11	.11	.11	.11	.11	.11	.10	.09	.08	.07	.05	.04	.03	.02	.01	.00	.00	.00	.00	.00	.00	.00	.00	.00	.01	.01	.02	.03	80
75	.13	.16	.18	.20	.22	.24	.25	.26	.27	.27	.28	.28	.29	.28	.28	.26	.23	.20	.16	.13	.09	.06	.03	.02	.01	.01	.00	.00	.00	.01	.01	.02	.03	.05	.08	.10	75
70	.32	.37	.42	.46	.48	.51	.52	.54	.55	.57	.58	.60	.61	.62	.61	.59	.55	.49	.41	.32	.24	.17	.10	.06	.03	.02	.01	.00	.01	.02	.03	.06	.10	.15	.20	.26	70
65	.67	.76	.83	.89	.95	.98	1.02	1.05	1.10	1.12	1.15	1.17	1.20	1.22	1.20	1.17	1.10	.99	.85	.70	.54	.39	.27	.17	.10	.06	.04	.04	.04	.06	.10	.16	.25	.35	.46	.57	65
60	1.25	1.40	1.50	1.57	1.65	1.70	1.75	1.85	1.95	2.00	2.05	2.10	2.15	2.22	2.25	2.22	2.17	1.95	1.62	1.35	1.05	.79	.58	.40	.27	.18	.14	.12	.14	.18	.26	.38	.53	.75	.95	1.13	60
55	2.22	2.42	2.57	2.68	2.75	2.82	2.85	2.87	2.90	2.95	3.05	3.20	3.28	3.33	3.30	3.27	3.10	2.95	2.55	2.12	1.72	1.37	1.09	.80	.58	.43	.34	.30	.32	.40	.54	.74	1.01	1.32	1.67	2.00	55
50	3.50	3.78	3.90	3.95	4.00	4.05	4.25	4.45	4.65	4.80	4.90	4.95	5.00	5.05	4.85	4.80	4.67	4.45	4.12	3.52	2.85	2.35	1.90	1.45	1.10	.85	.69	.62	.64	.76	1.00	1.40	1.85	2.25	2.65	3.05	50
45	5.00	5.20	5.35	5.40	5.45	5.55	5.65	5.80	6.00	6.22	6.38	6.55	6.77	6.95	7.05	6.85	6.55	6.10	5.50	4.87	4.25	3.68	3.08	2.55	2.00	1.60	1.35	1.15	1.15	1.40	1.80	2.35	3.05	3.70	4.25	4.70	45
40	6.95	7.15	7.37	7.52	7.80	8.25	8.57	8.90	9.15	9.32	9.45	9.55	9.75	9.95	9.85	9.25	8.62	7.95	7.20	6.40	5.45	4.80	4.22	3.75	3.10	2.60	2.20	1.90	1.95	2.25	2.65	3.32	4.25	5.15	5.90	6.55	40
35	9.47	9.65	9.98	10.43	10.87	11.33	11.72	12.07	12.35	12.55	12.65	12.65	12.35	11.95	11.50	11.00	10.40	9.75	9.32	8.77	8.15	7.20	6.22	5.30	4.50	3.80	3.25	2.90	2.85	3.10	3.70	4.75	6.45	7.40	8.95	9.35	35
30	11.45	11.70	12.05	12.47	13.02	13.55	13.85	14.25	14.45	14.55	14.45	14.35	14.20	13.95	13.55	13.15	12.65	11.85	11.15	10.67	10.15	9.45	8.42	7.40	6.30	5.35	4.55	4.00	4.00	4.20	4.95	6.90	8.92	10.37	10.75	11.10	30
25	13.10	13.60	14.05	14.40	14.72	14.95	15.30	15.65	15.95	15.98	15.85	15.55	15.27	14.90	14.55	14.15	13.72	13.25	12.87	12.52	12.15	11.65	10.95	9.85	8.55	7.20	6.05	5.30	5.25	5.85	7.35	9.45	11.25	11.82	12.25	12.65	25
20	14.20	14.60	14.95	15.30	15.65	16.05	16.40	16.75	16.95	16.95	16.70	16.45	16.10	15.75	15.35	14.95	14.55	14.15	13.85	13.55	13.25	12.85	12.40	11.60	10.65	9.30	7.95	6.90	6.75	7.47	9.10	11.22	12.45	13.05	13.45	13.85	20
15	14.86	15.20	15.51	15.85	16.21	16.63	17.02	17.31	17.51	17.50	17.28	16.99	16.58	16.18	15.85	15.50	15.15	14.80	14.55	14.30	14.05	13.75	13.35	12.90	12.15	11.20	10.00	8.85	8.60	9.75	11.70	12.45	13.15	13.65	14.10	14.50	15
10	14.98	15.31	15.65	16.00	16.39	16.81	17.20	17.50	17.73	17.66	17.51	17.23	16.86	16.52	16.20	15.91	15.64	15.37	15.10	14.85	14.65	14.40	14.10	13.75	13.25	12.60	11.80	11.05	10.95	11.65	12.45	13.10	13.64	14.00	14.32	14.64	10
5	14.77	15.04	15.40	15.78	16.20	16.64	17.03	17.32	17.53	17.53	17.40	17.19	16.90	16.61	16.32	16.10	15.88	15.67	15.46	15.27	15.07	14.83	14.55	14.25	13.95	13.45	12.90	12.40	12.30	12.69	13.10	13.47	13.79	14.00	14.24	14.48	5
0	14.20	14.50	14.75	15.15	15.45	15.90	16.35	16.70	17.00	17.15	17.00	16.81	16.61	16.40	16.16	16.02	15.90	15.77	15.60	15.41	15.21	15.01	14.80	14.60	14.30	13.97	13.61	13.29	13.10	13.14	13.35	13.54	13.70	13.79	13.92	14.00	0
− 5	13.50	13.70	13.96	14.25	14.60	15.00	15.45	15.85	16.07	16.20	16.20	16.15	16.05	15.95	15.85	15.75	15.65	15.56	15.45	15.32	15.17	15.00	14.82	14.64	14.40	14.15	13.85	13.57	13.39	13.31	13.36	13.40	13.42	13.36	13.35	13.40	− 5
−10	12.42	12.60	12.85	13.20	13.55	13.95	14.30	14.55	14.75	14.90	15.00	15.05	15.03	14.97	14.95	14.97	15.03	15.05	15.00	14.90	14.85	14.70	14.60	14.50	14.33	14.11	13.85	13.59	13.39	13.23	13.18	13.09	12.95	12.75	12.50	12.35	−10
−15	11.00	11.25	11.60	11.95	12.22	12.42	12.60	12.80	13.00	13.22	13.40	13.55	13.60	13.65	13.75	13.90	14.02	14.14	14.25	14.35	14.40	14.35	14.30	14.20	14.05	13.90	13.70	13.38	13.20	13.00	12.80	12.60	12.35	11.95	11.45	11.05	−15
−20	9.50	9.65	10.05	10.40	10.67	10.80	10.60	10.37	10.22	10.30	10.70	11.15	11.10	11.05	11.05	11.50	12.15	12.85	13.15	13.35	13.55	13.67	13.70	13.68	13.60	13.50	13.35	13.07	12.85	12.65	12.35	12.05	11.62	11.05	10.15	9.60	−20
−25	7.57	7.62	7.85	8.15	8.35	8.05	7.52	7.25	7.10	7.10	7.18	7.45	7.80	8.20	8.70	9.45	10.30	10.95	11.25	11.62	12.05	12.55	12.95	13.05	13.07	13.05	12.95	12.70	12.45	12.10	11.70	11.20	10.55	9.70	8.85	7.95	−25
−30	6.20	6.15	6.12	6.00	5.80	5.67	5.45	5.25	5.10	5.00	4.90	4.95	5.20	5.55	5.90	6.45	7.20	8.05	8.50	9.00	9.55	10.10	11.30	12.15	12.37	12.37	12.35	12.18	11.88	11.45	10.85	10.05	9.18	8.15	7.32	6.67	−30
−35	5.00	4.70	4.55	4.45	4.35	4.25	4.07	3.87	3.67	3.50	3.35	3.25	3.40	3.72	4.10	4.55	5.20	5.95	6.45	7.10	8.00	8.55	9.25	10.27	11.15	11.55	11.65	11.50	11.20	10.65	10.05	9.20	8.25	7.30	6.37	5.60	−35
−40	4.02	3.72	3.50	3.30	3.15	2.95	2.75	2.50	2.30	2.15	2.10	2.20	2.32	2.50	2.70	3.10	3.60	4.05	4.55	5.20	5.75	6.48	7.35	8.35	9.20	10.15	10.75	10.70	10.20	9.75	9.12	8.30	7.45	6.45	5.40	4.45	−40
−45	3.37	2.97	2.70	2.47	2.25	2.20	1.80	1.60	1.45	1.30	1.25	1.30	1.37	1.50	1.70	1.95	2.27	2.75	3.15	3.60	4.13	4.65	5.25	5.95	7.05	8.15	9.25	9.35	8.97	8.45	7.80	7.05	6.13	5.25	4.55	3.85	−45
−50	2.80	2.40	2.10	1.80	1.50	1.30	1.10	.89	.73	.61	.55	.54	.58	.67	.81	1.05	1.35	1.75	2.07	2.50	2.95	3.45	3.95	4.45	5.25	6.30	7.15	8.20	8.20	7.85	6.70	5.85	5.05	4.35	3.70	3.20	−50
−55	2.25	1.85	1.55	1.30	1.04	.85	.66	.50	.37	.28	.24	.22	.24	.28	.37	.50	.68	.92	1.20	1.55	1.90	2.30	2.80	3.35	3.90	4.55	5.15	5.52	5.60	5.45	5.10	4.67	4.15	3.65	3.10	2.60	−55
−60	1.70	1.40	1.15	.87	.68	.52	.38	.26	.17	.11	.08	.07	.07	.09	.14	.21	.32	.48	.67	.91	1.25	1.60	2.05	2.45	3.00	3.50	3.95	4.25	4.35	4.25	3.97	3.60	3.22	2.80	2.45	2.10	−60
−65	1.20	.95	.74	.57	.43	.31	.20	.13	.07	.04	.02	.01	.01	.02	.04	.07	.13	.22	.35	.51	.70	.93	1.20	1.49	1.90	2.25	2.60	2.83	2.95	3.00	2.90	2.70	2.42	2.15	1.88	1.55	−65
−70	.80	.64	.49	.37	.26	.18	.11	.06	.03	.02	.01	.01	.00	.00	.01	.02	.05	.10	.17	.27	.40	.55	.73	.93	1.12	1.35	1.57	1.75	1.87	1.90	1.87	1.77	1.58	1.37	1.15	.95	−70
−75	.52	.41	.31	.23	.16	.11	.05	.03	.02	.01	.00	.00	.00	.00	.00	.01	.02	.05	.09	.14	.22	.31	.42	.54	.67	.80	.92	1.01	1.08	1.11	1.10	1.05	.97	.87	.75	.63	−75
−80	.31	.25	.20	.16	.12	.06	.03	.02	.01	.00	.00	.00	.00	.00	.01	.02	.03	.04	.06	.09	.13	.18	.24	.30	.36	.43	.49	.54	.57	.59	.58	.57	.53	.48	.43	.37	−80
−85	.18	.16	.13	.11	.05	.03	.01	.00	.00	.00	.00	.00	.00	.00	.01	.01	.02	.03	.04	.05	.08	.10	.12	.14	.17	.20	.22	.24	.25	.26	.26	.26	.25	.24	.22	.20	−85

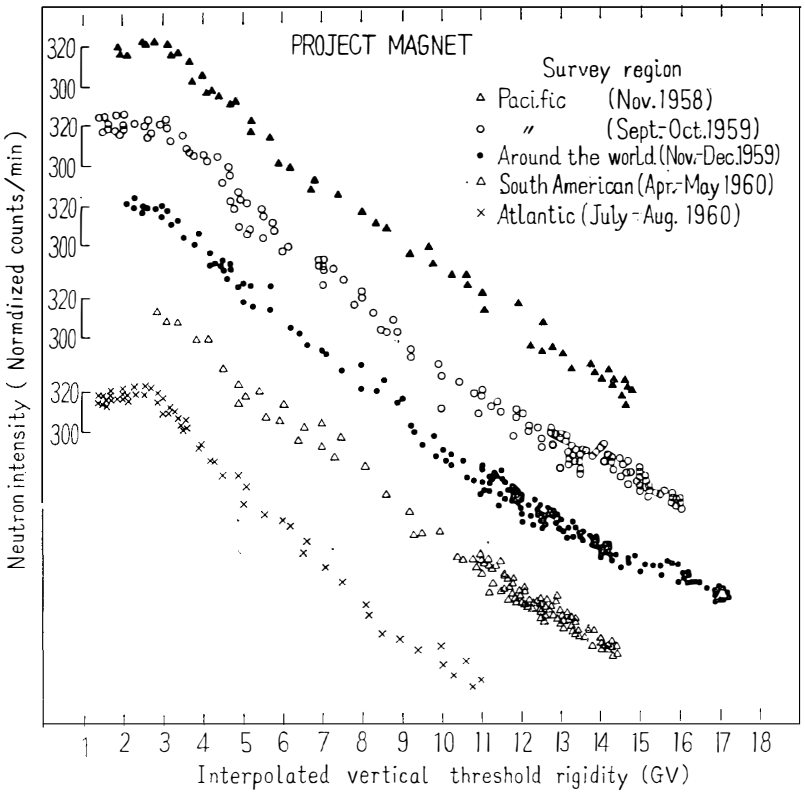

Fig. 22. Neutron intensities from the project 'Magnet' versus threshold rigidities interpolated using Table 7.

tion of the threshold rigidities was inconsistent with that of the observed cosmic ray intensities as seen in Fig. 13. The recent trailer survey by CARMICHAEL *et al.* (1965) in North America has furnished a valuable evidence to demonstrate such an inconsistency. To minimize the inconsistency, KONDO and KODAMA's (1965) table was revised a little.

Now, it is natural that the table ultimately derived, Table 7, involves inherent errors as described in preceding section 1. 3. To estimate these errors quantitatively, the threshold rigidities along the routes of the project 'Magnet' measurements were calculated from Table 7 by interpolation and were compared with results of neutron intensity measurements by POMERANTZ (1965). In Fig. 22, the observed neutron intensities are plotted against the interpolated threshold rigidities, separately in different survey routes. The r. m. s. deviation of the threshold rigidities more than 3 GV from a smoothed intensity-rigidity curve was found to be about 0.3 GV throughout the surveys, including the error of the measurements. Since the airborne survey routes were not coincident with the shipborne survey routes, the error of 0.3 GV may represent an upper limit of errors due to the non-uniform distribution of the data points used for prep-

Table 8. Interpolated and calculated threshold

Place	(A) Interpolated	(B) Calculated *	(A) − (B)
Ahmedabad	15.88	15.94	−0.06
Alma Ata	6.74	6.69	0.05
Apatity	0.61	0.64	−0.03
Bariloche	9.97	10.02	−0.05
Belgrano	0.74	0.75	−0.01
Bergen	1.14	1.13	0.01
Berkeley	4.51	4.50	0.01
† Brisbane	7.45	7.00	0.45
Budapest	4.43	4.44	−0.01
Buenos Aires	10.64	10.63	0.01
Calgary	1.08	1.09	−0.01
Cambridge	1.69	1.68	0.01
Cape Schmidt	0.57	0.60	−0.03
Chacaltaya	13.08	13.10	−0.02
Chamical	11.69	11.69	0.00
Chicago	1.79	1.72	0.07
Climax	3.04	3.03	0.01
College	0.52	0.54	−0.02
Cordoba	11.46	11.45	0.01
† Dallas	4.22	4.35	−0.13
Decepcion	3.50	3.55	−0.05
Deep River	1.00	1.02	−0.02
Denver	2.89	2.91	−0.02
Dunsink	2.08	2.08	0.00
Durham	1.42	1.41	0.01
Ellsworth	0.77	0.79	−0.02
Goose Bay	0.49	0.52	−0.03
Gottingen	3.08	3.00	0.08
Hafeleker	4.30	4.37	−0.07
Haleakala	13.32	13.30	0.02
Hermanus	4.87	4.90	−0.03
Huancayo	13.46	13.49	−0.03
Invercargill	1.90	1.86	0.04
† Irkutsk	3.98	3.74	0.24
Jungfraujoch	4.44	4.48	−0.04
Kampala	14.90	14.98	−0.08
Kerguelen	1.17	1.19	−0.02
Khartoum	15.55	15.56	−0.01
Kiel	2.38	2.29	0.09
Kiruna	0.52	0.54	−0.02
Kodaikanal	17.43	17.47	−0.04
Kronogard	0.64	0.69	−0.05
Lae	15.61	15.52	0.09
Leeds	2.17	2.20	−0.03
Lerwick	1.09	1.09	0.00
† Limeil	3.54	3.64	−0.10
Lincoln	2.29	2.22	0.07
Lindau	3.07	3.00	0.07

rigidities for cosmic ray stations.

Place	(A) Interpolated	(B) Calculated *	(A) − (B)
Lomnicky Stit	4.00	4.00	0.00
London	2.68	2.73	−0.05
Macquarie Islands	0.52	0.55	−0.03
Matienzo	3.01	3.01	0.00
Mexico City	9.46	9.53	−0.07
Mina Aguilar	12.50	12.51	−0.01
Minneapolis	1.43	1.39	0.04
Moscow	2.54	2.46	0.08
Mt. Norikura	11.62	11.39	0.23
Mt. Washington	1.23	1.24	−0.01
† Mt. Wellington	2.02	1.89	0.13
Munich	4.05	4.14	−0.09
Murmansk	0.50	0.50	0.00
Orsay	3.62	3.69	−0.07
Ottawa	1.07	1.08	−0.01
Oulu	0.80	0.81	−0.01
Palo Alto	4.64	4.73	−0.09
Pic du Midi	5.41	5.36	0.05
Point Barrow	0.23	0.24	−0.01
Posadas	11.62	11.64	−0.02
Prague	3.62	3.53	0.09
Reykjavik	0.39	0.41	−0.02
Rio de Janeiro	11.74	11.73	0.01
Rio Gallegos	7.39	7.31	0.08
† Rome	6.21	6.31	−0.10
Sacramento Peak	4.91	4.98	−0.07
SANAE	0.96	1.02	−0.06
Sulphur Mountain	1.11	1.14	−0.03
Sverdlovsk	2.39	2.30	0.09
Swarthmore	1.90	1.92	−0.02
Syowa	0.41	0.42	−0.01
Tbilisi	6.62	6.67	−0.05
Teheran	10.54	10.56	−0.02
Tixie Bay	0.49	0.53	−0.04
Trivandrum	17.41	17.44	−0.03
Tromso	0.38	0.41	−0.03
Tucuman	12.09	12.09	0.00
Uppsala	1.40	1.43	−0.03
Ushuaia	5.69	5.68	0.01
Utrecht	2.77	2.76	0.01
Victoria	1.91	1.86	0.05
Yakutsk	1.73	1.70	0.03
Zugspitze	4.26	4.24	0.02

* SHEA *et. al.*'s effective vertical threshold rigidities as calculated by 0.01 GV intervals.

† In this place (A)−(B) difference is more than 0.1 GV.

aration of the threshold rigidity table (SHEA and SMART, 1967).

Another test of Table 7 is made by comparing the threshold rigidities interpolated from the table with the values determined from 0.01 GV integration step calculation by SHEA *et al.* (1965b). The two sets of threshold rigidities for 91 cosmic ray stations are listed in Table 8. It can be seen that the difference between the two is fairly small, less than 0.1 GV, excepting only six stations marked by a symbol of †. The difference of 0.45 GV at Brisbane is the largest, but the interpolated value is almost the same with that calculated by 0.1 GV integration steps, just as the case in Irkutsk (KODAMA, 1965).

In middle latitudes where the penumbral effect is important, it is inevitable that the threshold rigidity is subject to errors greater than in other latitudes. A measure to see the latitude dependence of the error would be given by the width of the penumbral region determined from the trajectory calculations. When one defines both the main cone cutoff, P_m, above which all rigidities are allowed, and the Störmer cone cutoff, P_s, below which all rigidities are forbidden, the width of the penumbral region is defined as

$$\delta P = P_m - P_s. \tag{11}$$

In Figs. 23 and 24, values of δP calculated for specific locations are plotted as a function of the geomagnetic latitude and the threshold rigidity, respectively, together with SCHWARTZ's theoretical curve (1959). Distribution of δP in both figures seems to be directly related to a probable geographic dependency of the

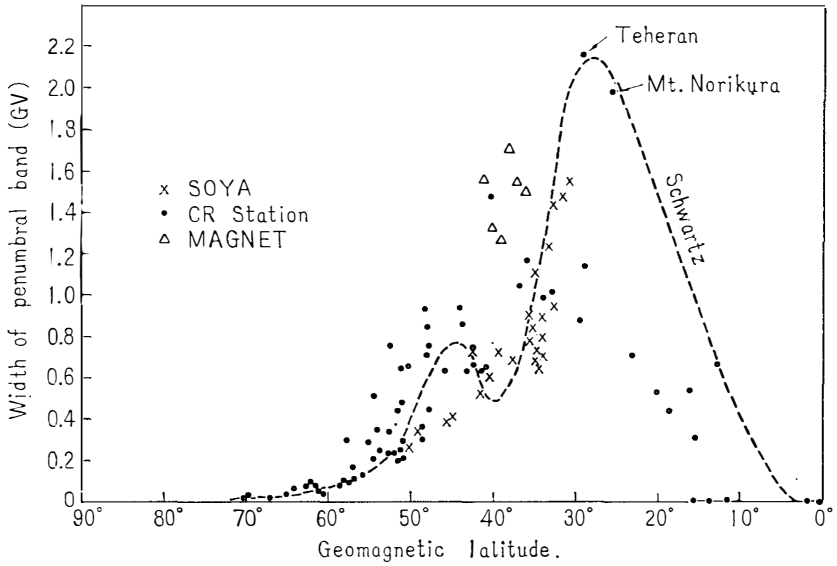

Fig. 23. A width of the penumbral region, defined by the difference between the main cone cutoff and the Störmer cone cutoff, is plotted against the geomagnetic latitude. The calculated widths are given for selected points from SOYA and 'Magnet' survey, and for all of the cosmic ray stations. The theoretical curve by SCHWARTZ is drawn.

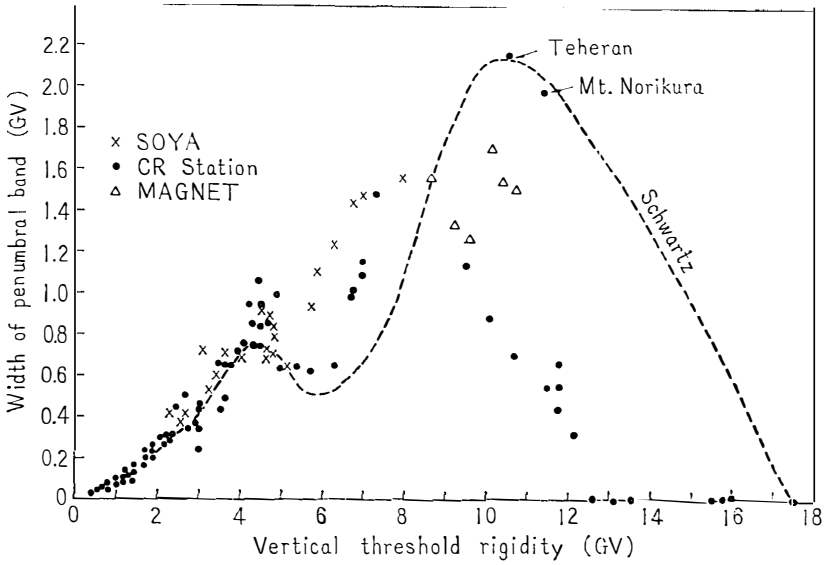

Fig. 24. A width of the penumbral region as plotted in Fig. 23 versus the trajectory-computed rigidity. The SCHWARTZ*'s curve is transfered from the curve of Fig. 23 by assuming* $P_c = 17.5 \cos^4\phi$.

penumbral errors involved in P_c deduced from the eq. (6). It is noticeable that only two points, Teheran and Mt. Norikura, are too far apart from the majority of points. This may be an absorbing question, though no physical interpretation can be given here.

In conclusion, the present threshold rigidity table will be useful for the determination of the effective threshold rigidity at any point on the earth, with the computation error of about 0.1 GV. However, considering physically the true significance of the errors, the threshold rigidity derived from Table 7 may involve an error of 0.3 GV or less ultimately, as proved from the comparison with cosmic ray measurements in Fig. 22, possibly due to the various ambiguities referring to penumbral corrections, inclined direction effects of cosmic ray particles, or geomagnetic field simulations.

1. 8. Concluding remarks

Using the data obtained from ten shipborne surveys for cosmic ray measurements during 1954–1962, the world-wide distribution of the cosmic ray intensity was examined in order to test the usefulness of the trajectory-computed vertical threshold rigidities. Summarizing all the results thus deduced, the following conclusions will be drawn.

1). The cosmic ray intensity *versus* the threshold rigidity curve can be ordered much better by use of the threshold rigidities determined by the trajectory calculations than by the QUENBY and WENK's values, which hitherto have given the best approximation among the different sets of values obtained analytically.

2). By comparison of the neutron intensities observed in regions of different longitude, it was found that the vertical threshold rigidities at several points in the Caribbean Sea may include a considerable error amounting to about 1 GV. This fact suggests the limitation of the usefulness of the vertical threshold rigidities proposed so far, even if the trajectory calculations were performed at 0.01 GV rigidity intervals.

3). A numerical table of the vertical threshold rigidities determined from trajectory calculations was prepared every 5° latitude and 10° longitude in geographic coordinates. The overall error involved in the threshold rigidity interpolated from the table can be estimated to be 0.3 GV or less, possibly due to the various ambiguities introduced in the following procedures: representation of the real geomagnetic field, including its secular change, corrections for the penumbral effect and the effect of cosmic ray particles from inclined directions.

4). The position of the cosmic ray equator, in 110°E–130°E, based on the sea-level data is 1.5° to 2.1° south of that of the maximum threshold rigidity equator, while the cosmie ray equator based on the airplane data coincides well with the theoretical one. But no explanation can be given of this controversial result.

5). In the vicinity of the intense geomagnetic anomaly near Cape Town, the sea-level neutron intensities evidenced the existence of an apparent latitude knee near 35°S in ordinary geomagnetic latitude, where it is not detectable at an airplane altitude of 640 g/cm^2. However, the position of the knee referred to the threshold rigidity is found identical between the different heights.

PART 2. SOLAR MODULATION OF COSMIC RAY LATITUDE VARIATION

2.1. Introduction

Among the various modulations of the galactic cosmic radiation the most remarkable is the intensity variation negatively correlated with the 11-year sunspot cycle. It is believed that a more or less low energy portion of the primary cosmic rays would be modulated by changes of the electromagnetic condition in the interplanetary space. SIMPSON (1962) suggested a heliocentric magnetic field boundary for the solar modulating region, possibly formed by an interface with the galactic magnetic field. If it is true, appreciable changes would be expectable not only in intensity but also in energy spectrum of the primary cosmic rays. In fact, numerous studies of the latitude effects of the cosmic ray intensity have shown that the cosmic ray spectrum is modulated with the solar cycle in energy region as would be affected by the geomagnetic field (MEYER and SIMPSON, 1958; NEHER and ANDERSON, 1960). Since a yearly change of the latitude variation is a direct measure to indicate solar modulating variations of cosmic ray intensity, investigations of it provide clues to the origin of the 11-year solar modulation mechanism. In such a research field, the threshold rigidity plays an important role for the determination of the rigidity spectrum of the various cosmic ray phenomena. However, analyses of the latitude variation to examine the solar modulation were scarecely made by using sea level data, but occasionally only by high altitude data giving a perceptible change in intensity rather than in sea level (POMERANTZ *et al.*, 1960; WINCKLER and PETERSON, 1958). In Part 2, it is tried to utilize the sea-level latitude variations deduced in Part 1, in order to obtain a year-to-year change of the response function for the neutron monitor.

On the other hand, there are a number of neutron monitor stations distributed over the world, supplying the continuous recording data useful for studies of cosmic ray time variations. To deduce the primary cosmic ray spectrum from these station data, the response function as derived from latitude surveys, corresponding to the observation time during a solar cycle, should be of great

necessity. On the contrary, it is worth comparing the 11-year variation of the response function with the spectral variation based on the station data. The latter is made as an extension of the study by KODAMA and WADA (1960), who examined the 11-year variation of the cosmic ray neutron intensity near the maximum of solar activity in 1957–58.

The negative correlation between the solar activity and the cosmic ray intensity is closely related to the displacement of the latitude knee (MEYER and SIMPSON, 1958). As in the case of the intensity-rigidity dependence, this displacement is detectable more prominently in high altitudes than at sea level. Indeed, no definite evidence of the displacement has been reported on the basis of sea level data. Also, the cosmic ray equator, another important property of the latitude variation, has been scarcely investigated with reference to the 11-year solar cycle. POMERANTZ *et al.* (1960) reported that the location of the cosmic ray equator at 14°W appears to have remained fixed within approximately 1° during 1956–58, but that the possibility of a small progressive change of about the magnitude of the uncertainty cannot be precluded. If the trajectories of cosmic ray particles are significantly affected by distortions of the geomagnetic field due to interactions with the interplanetary medium, then an observable shift of the cosmic ray equator may be expected during a solar cycle. In the following sections will be given descriptions of solar modulations of both the cosmic ray latitude knee and the cosmic ray equator observed in the SOYA surveys.

So far, various mechanisms have been proposed to account for the 11-year variation of the cosmic ray intensity. As reviewed by WEBBER (1962), whether the 11-year variation represents the effect of flux or energy modulation is a fundamental question concerning the theoretical models. PARKER (1958, 1963) proposed a model of the interplanetary magnetic field which may be disturbed by the outward flow of solar gas. This disordered magnetic field will shield the earth from the galactic cosmic rays. The efficiency of this screening effect depends upon a given field strength and the outward velocity of solar wind, *i. e.*, being the greatest at the solar maximum. ELLIOT *et al.* (1960) and DORMAN (1960) showed that the experimental results of the solar modulation are compatible with the solar wind model. But their studies were based on the data obtained from a limited number of cosmic ray stations which do not cover the entire rigidity range with continuous intervals. NAGASHIMA *et al.* (1966) concluded from an analysis of the recent satellite data that the solar wind model is preferable to the electric field modulation model by EHMERT (1960). The suitability of the solar wind model will be discussed in the light of the present response functions.

According to the results from the meson intensity recorded in shielded ion chambers, the 11-year variation appears to lag about a half year behind the solar activity when one uses the relative sunspot number as an index (FORBUSH, 1958). However, no clear evidence is still given with respect to the position of the latitude knee for the sea-level nucleonic component. The presently available survey

data will be analyzed for the study of this hysteresis effect.

The actual test for the suitability of the threshold rigidity and the response function can be made by applying them to the special cosmic ray event. In this work, the test will be made for two cases of the FORBUSH decrease of July, 1959 and the solar proton increase of February 23, 1956, which are typical examples of the solar modulations of the primary cosmic ray intensity.

2. 2. Cosmic ray equator

Since the expedition ship SOYA crossed, twice a voyage, the cosmic ray equator at 107°E geographic, the determination of the location of the cosmic ray intensity minimum was made ten times during 1956–1962. A summary of the observation results is given in Table 9. No experimental data was obtained on the two outbound voyages. These positions were determined by least squares fit of the polynominal function

$$y=\sum_{i=1}^{n}a_i x^i \qquad (12)$$

to the intensity *versus* latitude data between 35°N and 20°S geographic. Indeed, the effect of the choice of n from 2 to 5 upon the position of the minimum was not appreciable.

Table 9. Position of the cosmic ray minimum at 107°E observed on board the SOYA.

Survey No.	Outbound voyage		Homebound voyage	
	Date	Geographic latitude	Date	Geographic latitude
6	—	—	Apr. 4, 1957	6.7°N
7	Nov. 22, 1958	6.5°N	Apr. 3, 1959	7.5°N
8	—	—	Apr. 9, 1960	6.5°N
9	Nov. 22, 1960	6.4°N	Apr. 22, 1961	6.7°N
10	Nov. 8, 1961	6.2°N	Apr. 5, 1962	7.3°N
Average		6.4°N±0.1°		6.9°N±0.4°

As seen in Fig. 2, the year-to-year variation of the relative number of sunspots during the period from the first survey of the SOYA to the last one was predominent so that its magnitude amounted to about 80% of the full amplitude throughout a complete solar cycle. Therefore, a significant change of the position of the cosmic ray equator should be observed during this survey period if the position is dependent upon the level of solar activity. However, as seen in Table 9, the observed positions display no significant changes as correlated with solar activity, though a little seasonal variation may exist. Such a constancy of the cosmic ray equator found in the SOYA surveys suggests that no distortion of the geomagnetic field could be caused by interactions with the interplanetary

medium, and that if any, it gives no significant influence on the sea-level position of the cosmic ray equator.

2. 3. Cosmic ray latitude knee

In the SOYA surveys, the cosmic ray latitude knee was observed near 30°E geographic twice a voyage. As described in section 1. 6, the intensity *versus* latitude curve does not always represent the real latitude knee as closely related to solar activity, when the ordinary geomagnetic latitude based on the dipole term only is used. Therefore, it is meaningless to compare the positions of the latitude knees in different longitudes, so far as the conventional geomagnetic coordinates are concerned. Thus, it is physically significant to discuss the 11-year variation of the latitude knee in terms of the intensity-rigidity curve rather than the intensity-latitude one. Otherwise, HAKURA's (1965) corrected coordinates must be used for representation of the geomagnetic latitude, as mentioned earlier. In this work, neutron intensities were plotted as a function of the vertical threshold rigidities, and then the position of the knee on the intensity-rigidity curve was determined for each survey.

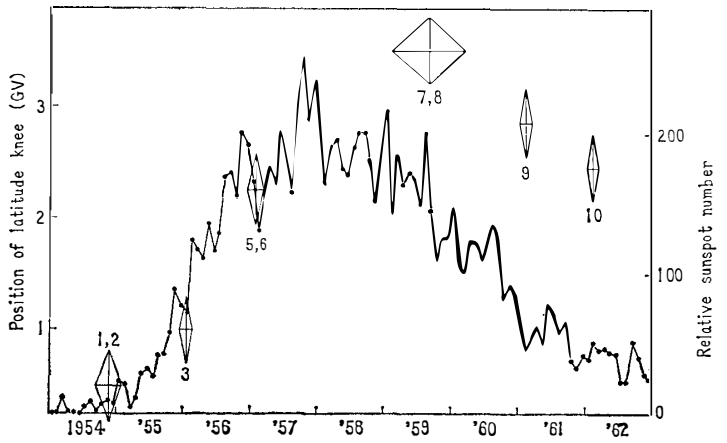

Fig. 25. Yearly changes in the position of the latitude knee (indicated by diamond marks) and the sunspot relative number. Attached figures are Survey No. designated in Table 1.

Similarily, data from the other ships, LABRADOR, ATAKA and ARNEB, were utilized for the determination of the position of the 'rigidity knee'. Summarizing all the results including that of the SOYA, the 11-year variation of the position of the 'rigidity knee' can be recognized clearly (cf. Figs. 26 and 27 in section 2. 4). That is, the position of the 'rigidity knee' moves toward a higher rigidity as solar activity increases, from about 1 GV to near 3 GV. The position found at the solar minimum of 1954 is almost identical with that in CARMICHAEL *et al.*'s (1965) trailer survey at the next solar minimum of 1965.

To represent quantitatively the position of the 'rigidity knee', we approximately define it by the method which will be described in section 2. 4. The positions thereby obtained are shown in Fig. 25, where the position of the 'rigidity knee' is indicated by a diamond mark attached by the survey No., and black circles show the Zürich sunspot relative numbers. The 11-year variation of the position of the 'rigidity knee' associated with solar activity is evident even at sea level. In addition, a slight tendency of the phase difference may be apparent between the position of the 'rigidity knee' and the relative number of sunspots. Though the exact determination of the difference is rather hard due to a considerable error included in the position, it is consistent with the result as suggested by FORBUSH (1958), *i. e.*, a definite time lag of cosmic ray intensity variation, approximately six months, from the 11-year variation of solar activity.

2. 4. Response functions for the sea-level nucleonic component

A variety of cosmic ray detectors are now in operation to measure time variations of cosmic ray intensity. In order to infer from the observed time variations the actual primary intensity variations taking place at the top of the atmosphere, it is necessary to know the differential response functions for the respective detectors corresponding to the observation period. Among the various detectors, the response function for the neutron monitor would be most available, because more than 100 neutron monitor stations are distributed over the world. Using the neutron data from the present latitude surveys, we can deduce the differential response function of the sea-level neutron monitor and its solar modulation.

The counting rate of the neutron monitor at time t_o located at an atmospheric depth of x g/cm^2, where the vertical threshold rigidity is P_c, is given by

$$N(P, x, t_o)=\int_{P_c}^{\infty} m(P, x)\, \frac{dJ}{dP}(P, t_o)\, dP, \qquad (13)$$

where (dJ/dP) (P, t_o) is the flux of particles of rigidity between P and $P+dP$ at time t_o, and $m(P, x)$ is the ratio of the number of particles recorded by the instrument that have originated from particles of rigidity between P and $P+dP$. m is the overall multiplicity. Then the differential response function, or the total differential counting rate of a detector, is defined by

$$\frac{dN}{dP}(P, x, t_o)=m(P, x)\, \frac{dJ}{dP}(P, t_o). \qquad (14)$$

The quantity $N(P, x, t_o)$ is given by the actual intensity-rigidity curve as determined from latitude surveys. In Fig. 26 five sets of the intensity-rigidity curves were fitted, with the least square method of the polynominal function, to observation points of each of the SOYA surveys. Also, another five sets of curves, from LABRADOR, ATKA, LEIPZIG and ARNEB, were shown in Fig. 27, where a small part of the vertical threshold rigidities were derived from Table 7.

At a different time t, at the same atmospheric depth at a location of the

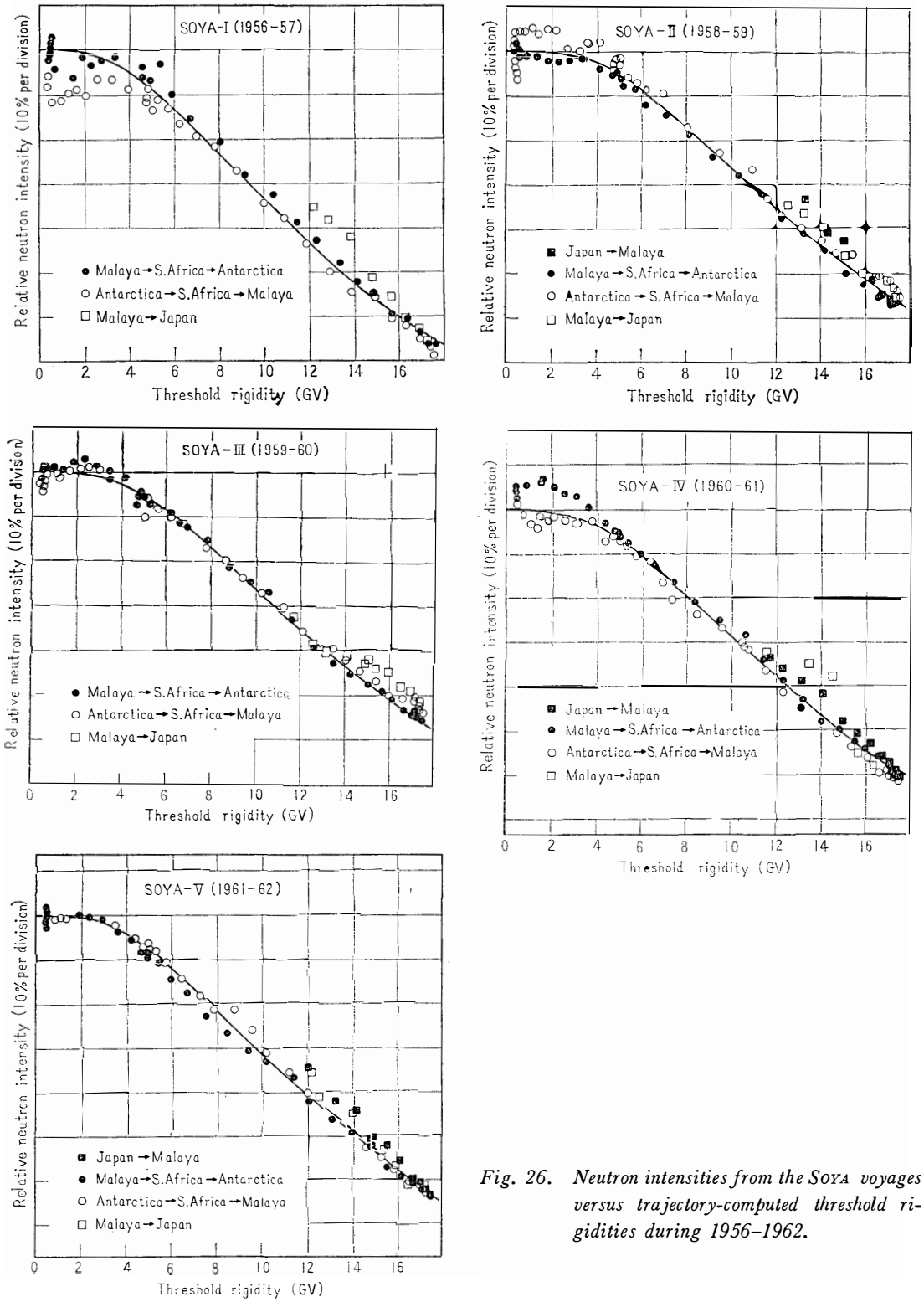

Fig. 26. Neutron intensities from the SOYA voyages versus trajectory-computed threshold rigidities during 1956–1962.

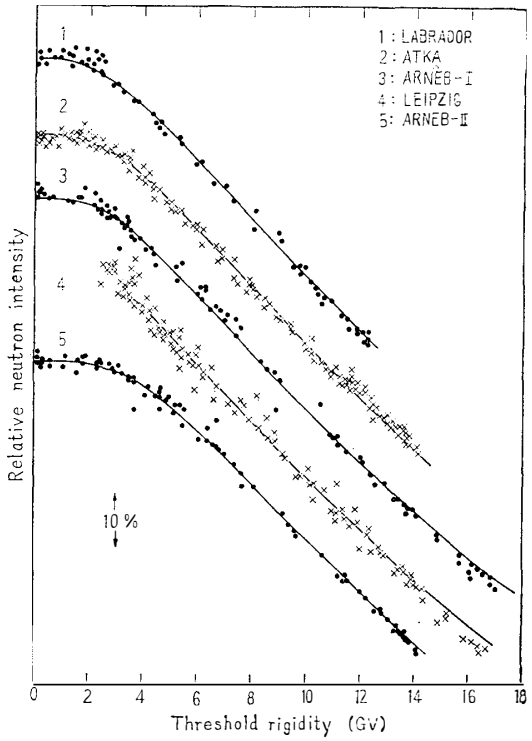

Fig. 27. Neutron intensities from the LABRADOR, ATKA, LEIPZIG *and* ARNEB *voyages versus trajectory-computed threshold rigidities.*

same threshold rigidity, the counting rate is

$$N(P, x, t)=\int_{P_c}^{\infty} m(P, x)\frac{dJ}{dP}(P, t)\,dP\,. \tag{15}$$

From the eqs. (14) and (15),

$$\frac{\frac{dJ}{dP}(P, t_0)-\frac{dJ}{dP}(P, t)}{\frac{dJ}{dP}(P, t_0)}=\frac{\frac{dN}{dP}(P_c, t_0)-\frac{dN}{dP}(P_c, t)}{\frac{dN}{dP}(P_c, t_0)}\,. \tag{16}$$

The right-hand side of the equation is easily determined from any two curves of Figs. 26 and 27. The left-hand side gives the fractional decrease in the primary flux. No assumption as to the energy spectrum of primary radiation is necessary. This indeed is the advantage of using the latitude surveys in two different periods.

In the above equations, no distinction has been made as to the charges on different nuclei in the primary spectrum. This is justified at a first approximation, since the rigidity spectra of different nuclei are similar, and WEBBER (1962) has shown protons and α particles are modulated in a similar fashion, *i.e.*, the modulation of primary particles is independent of their charge. It should be considered that the results given here refer to the overall flux of the primary particles.

The neutron monitors actually used in the latitude surveys in different phases of the solar cycle were those of having a similar geometry but were not identical, hence their absolute counting rate were not always the same throughout the

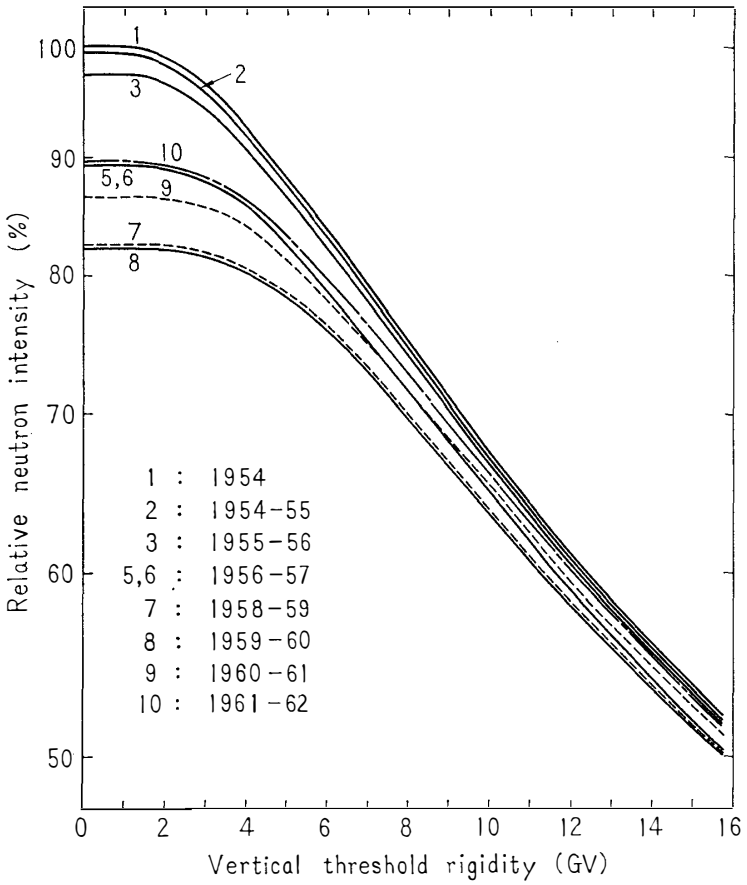

Fig. 28. Year-to-year change of normalized intensity-rigidity curves of the sea-level nucleonic component, in terms of trajectory computed threshold rigidity.

whole survey period. Therefore, before the data from ten sets of the intensity-rigidity curves are compared, they have to be normalized with the data from a neutron monitor that was in continuous operation covering the periods of latitude surveys adopted in this work. MATHEWS and KODAMA (1964) referred to the neutron monitor at Mt. Washington. But, to avoid a probable altitude dependence of time variations, the data from Chicago, of which threshold rigidity is 1.72 GV, was adopted in place of Mt. Washington. Hence, the neutron intensity at 1.72 GV observed in a given survey was normalized to the intensity at Chicago corresponding to the time of the survey. The intensity-rigidity curves thus normalized are shown in Fig. 28, where attached figures indicate the survey No. listed in Table 1. For convenience, all values of the neutron intensities are converted relative to a value of 100.0 at 15 GV in 1954 and tabulated in Table 10. Then the values of dN/dP were determined as a function of rigidity, and are shown in Fig. 29.

The fractional decrease of the primary flux at the time of the latitude survey from the flux at the solar minimum of 1954, that is, the solar cycle modulation of the total primary flux as a function of rigidity, is given by the eq. (16).

Table 10. Integral response function for nucleonic component at sea level during 1954–1962.

Survey No.	1	2	3	5,6	7	8	9	10
Rigidity \ Year	1954	1954–55	1955–56	1956–57	1958–59	1959–60	1960–61	1961–62
1 GV.	188.2	185.9	182.1	167.1	155.4	153.6	161.5	167.9
2	185.5	183.6	180.2	166.2	154.9	153.2	160.9	167.1
3	179.9	178.5	175.7	163.9	153.6	152.1	159.3	165.1
4	172.6	171.5	169.3	159.7	151.4	150.0	156.5	161.4
5	164.4	163.6	161.7	153.9	147.4	146.3	152.0	156.0
6	156.0	155.4	153.8	147.3	142.3	141.5	146.3	149.7
7	147.8	147.2	145.9	140.4	136.6	136.0	140.1	142.9
8	140.0	139.5	138.4	133.6	130.7	130.2	133.8	136.1
9	132.7	132.2	131.2	127.1	124.9	124.4	127.6	129.6
10	125.9	125.5	124.6	120.9	119.2	118.9	121.7	123.4
11	119.7	119.3	118.5	115.2	114.0	113.6	116.4	117.7
12	114.0	113.7	113.0	109.9	109.0	108.7	111.2	112.4
13	108.9	108.6	107.9	106.1	104.4	104.2	106.4	107.5
14	104.2	103.9	103.3	100.6	100.2	100.0	102.0	103.0
15	100.0	99.7	99.1	96.6	96.3	96.1	98.0	98.9
16	96.2	95.9	95.3	92.9	92.7	92.6	94.4	95.2
17	92.7	92.4	91.9	89.6	89.5	89.4	91.1	91.8

All values are relative to 100.0 at 15 GV in 1954.

Fig. 30 illustrates thus obtained results, where double dashed lines show the magnitude of the overall error accompanied with the lowest curve (No. 7, 8) close to the solar maximum. These curves represent the spectral response of the modulating mechanism responsible for producing the 11-year solar cycle intensity variation at sea level.

In Fig. 30, it appears that the lower rigidity particles begin to decrease as solar activity increases and that particles below 2 GV are almost entirely removed from the primary radiation at the solar maximum. For neutrons, the atmospheric cutoff is about 1 GV, *i.e.*, a sea level neutron monitor is not sensitive to particles of this rigidity, hence the results should not be considered very reliable at the low rigidity end of the spectrum. However, above 3 GV, the neutron monitor gives excellent results.

The uncertainty in the experimental data and the threshold rigidities used causes scattering of points as seen in Figs. 26 and 27. As a result, we estimate from the r. m. s. scatter the resulting error in final results to be 0.3 GV in rigidity and 0.8% in intensity. Other sources of errors, such as the effect of possible differences in the neutron multiplicity distribution in the different piles and solar cycle variation of the atmospheric pressure coefficient, are minimized by the

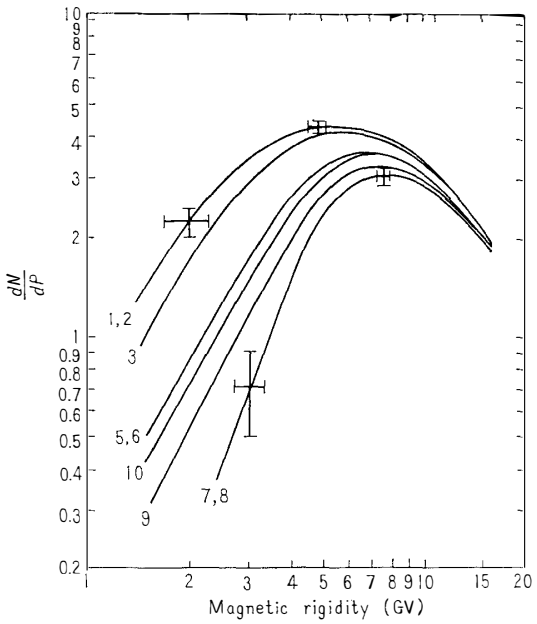

Fig. 29. Differential response curves, dN/dP, of the sea-level nucleonic component for different phases during 1954–1962. Attached figures mean Survey No. listed in Table 1.

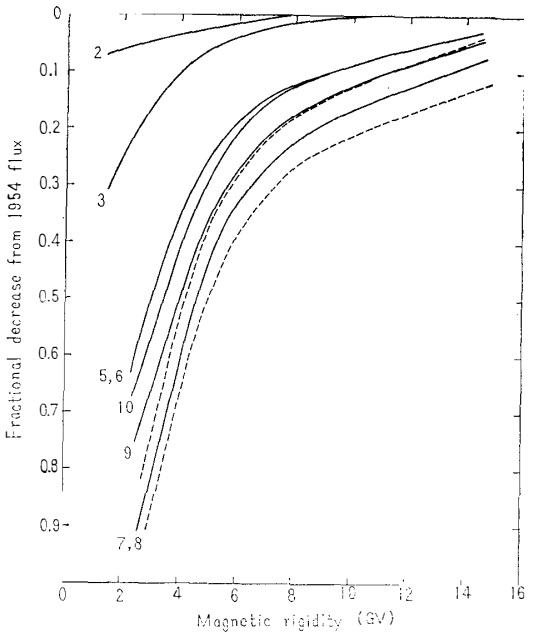

Fig. 30. Fractional decreases in primary cosmic ray flux plotted as a function of the threshold rigidities. Double dashed lines show the overall error for lowest curve No. 7, 8. Figures attached are Survey No. listed in Table 1.

normalization procedure. The latitude variation of the pressure coefficient is not expected to be large. The errors due to these three causes are estimated to be less than 5%.

The difference in a slope of the integral response function between the ascending and the descending phases of the solar cycle can be clearly seen in Fig. 28. For example, it is apparent in a comparison between the curves No. 3 and No. 9, corresponding to almost the same level of solar activity as shown by the sunspot relative number in Fig. 2. This phenomenon is the very hysteresis effect as already reported on the basis of the long term variation of the cosmic ray intensity at a fixed station.

2. 5. Comparison of the response function with neutron monitor data obtained from fixed stations

When one compares the response function derived from latitude surveys with that from fixed observatories distributed over the world, it is convenient to substitute the integral response function by the amount of relative intensity variation,

$$\frac{\Delta N}{N}(P, t_0, t)=[N(P, t_0)-N(P, t)]/N(P, t_0). \qquad (17)$$

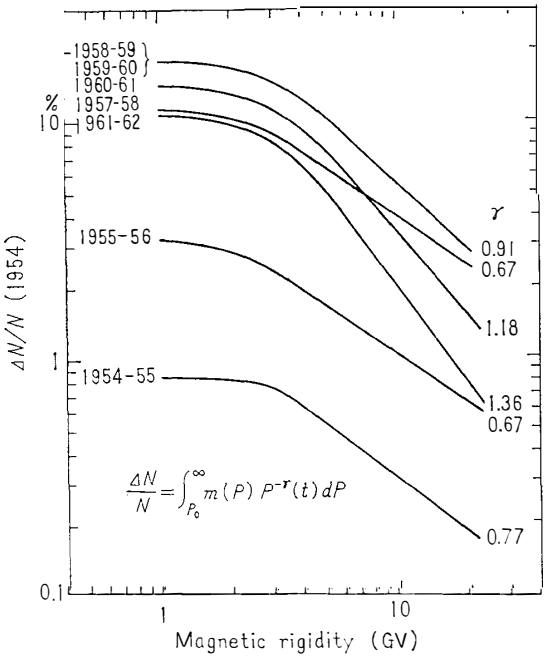

Fig. 31. Rigidity dependences of neutron intensity variations relative to 1954 flux, for different phases during 1954–1962.

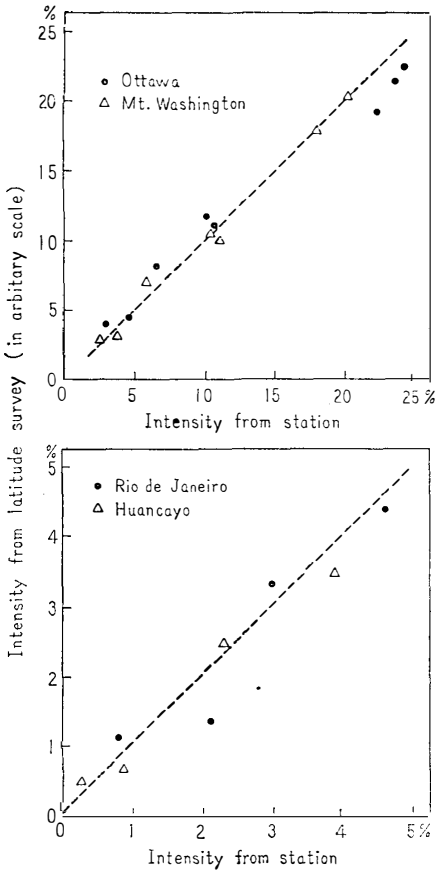

Fig. 32. Correlation between neutron intensities observed at fixed stations and those derived from the response functions. Yearly mean values from sea level and mountain sites in almost the same rigidity are plotted during 1954–1962.

Table 11. List of cosmic ray stations, neutron data of which were used to deduce the long term variation of cosmic ray intensity.

Station name	Altitude (m)	Threshold rigidity*
Deep River	—	1.02 GV
Ottawa	—	1.08
Sulphur Mountain	2283	1.14
Mt. Washington	1917	1.24
Chicago	—	1.72
Mt. Wellington	725	1.89
Climax	3400	3.03
München	—	4.14
Zugspitze	2960	4.24
Hermanus	—	4.90
Uppsala	—	5.68
Mt. Norikura	2770	11.39
Rio de Janeiro	—	11.73
Huancayo	3400	13.49

* Values by SHEA *et al.* (1965b).

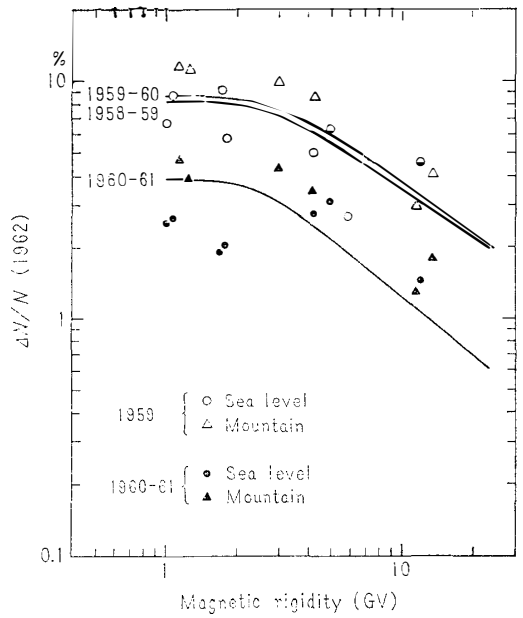

Fig. 33. A comparison of the rigidity dependence of the long term variation derived from the response functions with that based on fixed station data in different phases during a solar cycle.

This is because that direct comparisons among cosmic ray data from fixed stations are impossible in absolute intensity but possible in relative. For example, the values of $\Delta N/N$ are shown as functions of rigidity and time in Fig. 31, when the flux in the solar minimum of 1954 is taken as a standard level. These can be compared directly with the rigidity spectrum of the fractional intensity variations as deduced using the station data.

In order to check a consistency between the latitude survey data and the station data, 14 stations, listed in Table 11, were selected and then the long term variation of the cosmic ray neutron intensity was deduced following the method of the Ottawa group which removes the transient part of intensity variations such as FORBUSH decrease by connecting adjacent maximum points of daily mean values (FENTON *et al.*, 1958; KODAMA and WADA, 1960). In Fig. 32, the fractional intensity variation, $\Delta N/N(P, 1954, t)$, during the last solar cycle is plotted against that observed at each of the following four stations: Ottawa, Mt. Washington, Rio de Janeiro and Huancayo. The upper and the lower diagrams correspond to the lower and the higher parts of rigidity, respectively. In both cases, a good correlation is found between the station intensity and that derived from the response function, with the same proportion of variation. The altitude dependence of the long term variation, that is, the difference in the amount of intensity variation between the sea level and the mountain sites is not significant.

Since most of the cosmic ray stations started before and after the International Geophysical Year 1957–58, we can not deduce $\Delta N/N$ (P, 1954, t) from the present station data. Hence, the intensity variation normalized to the level in the last survey period of 1962, $\Delta N/N$ (P, 1962, t), was deduced. The variation function of $\Delta N/N$ (P, 1962, t) based on the response function was computed for three different periods, 1958–59, 1959–60 and 1960–61, and is shown in Fig. 33 with the station data. Different marks discriminate between the sea level and the mountain sites to look at a possible altitude dependence of the intensity variation. It is evident that a general consistency is recognized between the variation functions derived from two different kinds of cosmic ray data. Thus, both results show essentially the same property of the solar modulation in the rigidity spectrum variation.

However, the station data points greatly deviate from the curve, particularly in the case of 1960-61. As the roigins of such deviations, the following three could be considered.

1. Altitude dependence

As seen in Fig. 33, the intensity variations observed in the mountain stations are more conspicuous than in the sea level stations, in the rigidities less than about 5 GV.

2. Changes in the absolute level of flux

In general, it is not so easy to keep the observation conditions constant for cosmic ray measurements during a very long period. A certain degree of fluctuations in the absolute intensity would be inevitable due to instrumental troubles, or changes in the environment of the observatory.

3. Reduction of data

Various ambiguities would be introduced in process of corrections for the short term variation and the barometric pressure.

For the above reasons, it is concluded that the station data would be rather inadequate for the determination of the variation function, which can be deduced from the latitude survey data with better accuracy.

2. 6. Comparison of the response function with PARKER's solar wind model

According to PARKER's solar wind modulation model for the 11-year variation, the cosmic ray intensity near the earth at a time t_o, with a given magnetic rigidity P, is expressed by

$$j_e(P, t_o) = j_\infty(P, t_o) \exp\left[-M(P, t_o)/\beta\right], \tag{18}$$

where $j_\infty(P, t_o)$ is the correspoding intensity in the interplanetary space and β is the ratio of the particle velocity to that of the light. $M(P, t_o)$, the so-called modulation coefficient, is given by

$$M(P, t_o) = \begin{cases} a_0 & \text{for } P \leq P_1 \\ a_0 \left(\dfrac{P_1}{P}\right)^{-2} = b_0 P^{-2} & \text{for } P > P_1, \end{cases} \tag{19}$$

where a_0 is functions of the wind velocity, the number of collisions of a cosmic ray particle with scattering centers in the space and the light velocity. P_1 is a critical rigidity, at which the gyroradius of the particle is comparable to the linear dimension of the scattering center. Similarily, the cosmic ray intensity at a different time t is given by

$$j_e(P, t_o) = j_\infty(P, t) \exp\left[-M(P, t)/\beta\right]. \tag{20}$$

Denoting a ratio $j_e(P, t_o)/j_e(P, t)$ by R,

$$lnR = \begin{cases} \Delta a/\beta & \text{for } P \leq P_1 \\ \Delta b P^{-2}/\beta & \text{for } P > P_1, \end{cases} \tag{21}$$

where $\Delta a = a_o - a$ and $\Delta b = b_o - b$.

Thus a plot of lnR as a function of P on a logarithmic scale is advanta-

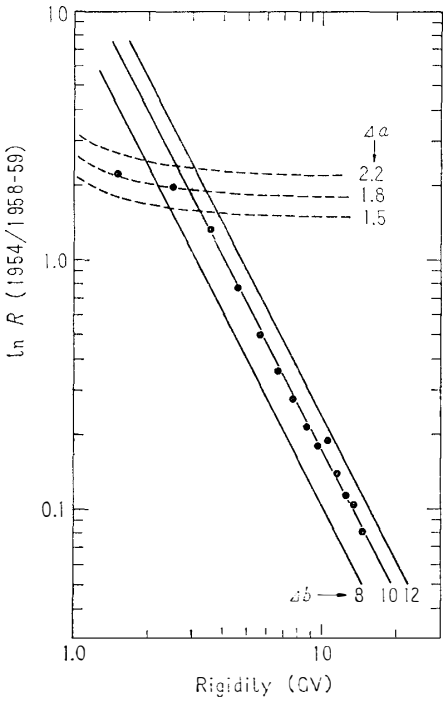

Fig. 34. Natural logarithms of the ratio R of the differential response function of 1954 to that of 1959 plotted as a function of rigidity. Curves are given according to PARKER*'s solar wind modulation theory.*

geous for a comparison between the exprimental results and the theoretical predictions. One example of the value of lnR derived from the present response function, the ratio of 1954 flux to 1958–59 flux, is shown in Fig. 34. Then, we can determine the theoretical curves best fitted to the observation points, separately in both sides of P_1, resulting in $\Delta a = 1.8$ and $\Delta b = 10$. Values of Δa and Δb, obtained by the similar procedure in different phases of the solar cycle, are summarized in Table 12. The 11-year variation of the response function at sea level appears to be consistent with the predictions by the solar wind theory.

It will be of interest to compare the above results with those obtained by satellite and balloon experiments, by which we can detect directly not only primary protons but also heavy nuclei components in the lower rigidity range (NAGASHIMA *et al.*, 1966; GLOECKLER and JOKIPII, 1966). In Fig. 35, the result obtained by NAGASHIMA *et al.* is reproduced. The observations in balloon flights, as indicated by black circles, characterize the epochs during which the data were acquired by Explorer VII and Ariel I satellites (cf. Fig. 1). The theoretical lines for different values of Δa and Δb are also drawn in the figure. The best fitted value of the modulation coefficient is found to be 0.4~0.5 and 20~24 for Δa and Δb, respectively, while 0.5 and 8 for the sea level measurements close to the cor-

Table 12. Modulation coefficients deduced from the response functions relative to that of 1954.

Period	Δa	Δb	P_1(GV)
1954–1955	0.02	0.5	2
1955–1956	0.3	1.2	2
1956–1957	0.9	5	3
1958–1959	1.8	10	4
1959–1960	1.8	10	5
1960–1961	1.3	8	4
1961–1962	1.0	6	3

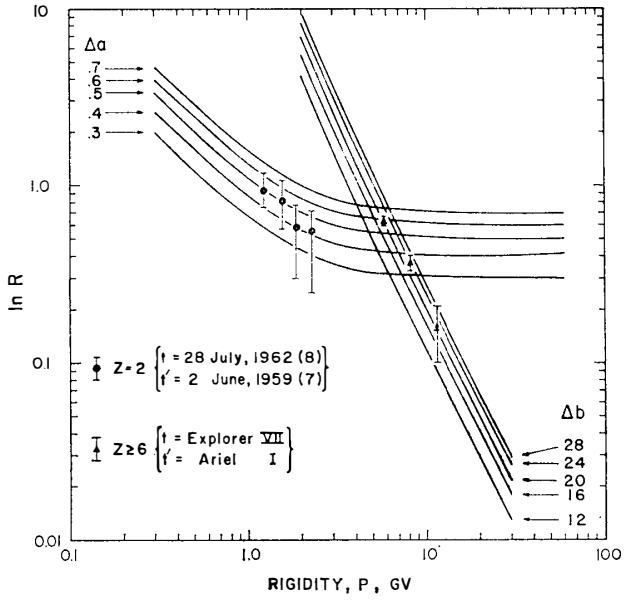

Fig. 35. Comparison of experimental lnR versus rigidity data with curves calculated on the basis of solar wind modulation theory (reproduced from NAGASHIMA *et al., 1966).*

responding epochs. It is concluded that the long term modulating mechanism for the heavy nuclei components of $Z \geq 6$ is a few times as large in efficiency as that for the sea level nucleonic component.

According to the energy modulation theory by the electric field (EHMERT, 1960), lnR can be approximated by

$$lnR \propto \Delta E/E,$$

where E is the total energy per nucleon, $\Delta E = \delta E(t_0) - \delta E(t)$, and $\delta E(t)$ is the energy loss at a time t (NAGASHIMA *et al.*, 1966). Since the observed lnR is proportional to P^{-2} or E^{-2}, the energy modulation theory is not suitable for the interpretation of the present sea-level observations, if ΔE is assumed to be constant over the entire spectrum.

2. 7. Application of the threshold rigidities and the response functions to other observation results

During the last solar cycle of 1954–1964, a number of cosmic ray phenomena showing remarkable intensity variations occurred, among which the most prominent one was the FORBUSH event comprising the three successive decreses in July, 1959, and another one was the solar proton event of February 23, 1956. Although numerous studies have been made of these special events, it is still worthwhile to discuss the rigidity spectrum of the intensity variations on the basis of the presently available threshold rigidities and response functions.

2. 7. 1. FORBUSH decrease in July, 1959

In order to determine the rigidity spectrum of this event, the bihourly values of cosmic ray data from 30 neutron monitor stations were used through July 9–

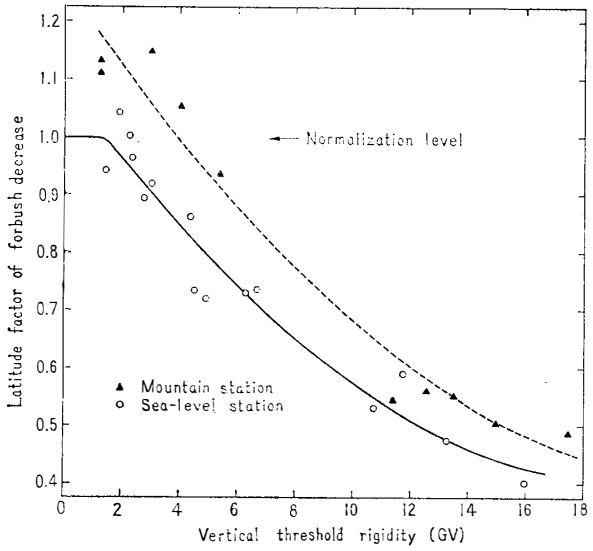

Fig. 36. Intensity decreases versus rigidity in the FORBUSH event of July, 1959, when neutron data from 30 cosmic ray stations were used.

25, excepting July 17 and 18 when some enhancements of solar protons happened to occur. A standard time variation during this period was deduced from the average of five sea-level high latitude stations: Thule, Resolute, Mawson, Churchill and Deep River. It gives $\Delta I = 21.7\%$ as the amount of the maximum bihourly

Table 13. Latitude factor, F, in the FORBUSH event of July, 1959.

Rigidity	Sea level	Mountain (760g/cm²)	Altitude factor
1 GV	1.000	—	—
2	0.963	1.125	1.17
3	0.903	1.056	〃
4	0.847	0.993	〃
5	0.792	0.934	1.18
6	0.742	0.878	〃
7	0.695	0.824	〃
8	0.650	0.773	1.19
9	0.611	0.726	〃
10	0.574	0.682	〃
11	0.540	0.640	〃
12	0.508	0.601	1.18
13	0.483	0.566	1.17
14	0.459	0.534	1.16
15	0.441	0.508	1.15
16	0.426	0.482	1.13
17	0.415	0.462	1.11

All values are relative to 1.000 at 1 GV at sea level.

decrement from the pre-event intensity level. The minimum intensity was found at 20h–22h U. T. of July 15 and the pre-event level was taken as an average intensity from 0h of July 9 to 15h on 11th.

Denoting bihourly values of the standard variation by $N_0(t)$, and those for other individual stations by $N(t)$, the latitude factor, F, was calculated so as to minimize the following quantity:

$$\sqrt{\{[(F\cdot N_0(t_1)-N(t_1))^2+(F\cdot N_0(t_2)-N(t_2)+\cdots\cdots+(F\cdot N_0(t_{180})-N(t_{180}))^2]/180\}},$$

where 180 bihourly values were used, since this event covered 15 days. In Fig. 36, F values thus obtained for 15 sea level and 10 mountain stations* are plotted as a function of the vertical threshold rigidities respectively. It can be seen that the altitude dependence is apparent. From the least square curves fitted to observation points, the altitude factor, *i.e.*, the ratio of F values between the sea level and a depth of 760 g/cm^2 was found to be about 1.18 in the rigidity range of 1–13 GV. The least square fitted values of F and their altitude factor are given in Table 13.

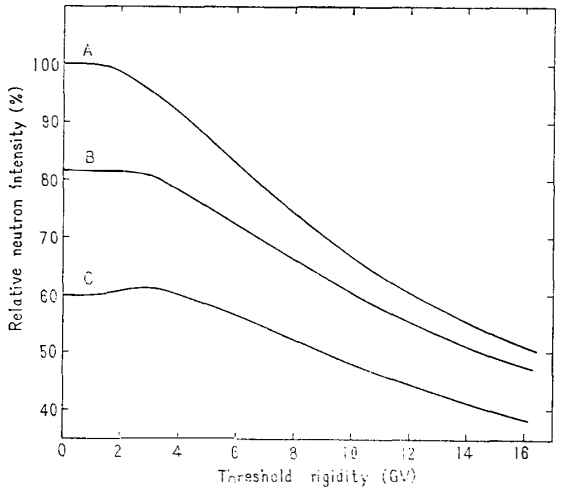

Fig. 37. Normalized cosmic ray neutrou intensities versus threshold rigidities. Curves A (solar minimum, 1954) and B (solar maximum, 1959) are deduced from latitude surveys, and curve C corresponds to the FORBUSH *decrease of July, 1959.*

Since the normal response curve is given for the time of the solar maximum during which this event occurred, one can deduce the intensity-rigidity curve expected at the bottom of the event in progress. In Fig. 37, two curves A and B are the normalized response functions corresponding to the periods of the solar minimum, 1954, and the maximum, 1959. Subtracting $F\cdot\Delta I$ values, using sea-level curve of Fig. 36, from curve B results in curve C.

From the difference between curves B and C in Fig. 37, we can deduce the fractional decrease of this FORBUSH event as a function of rigidity by a similar process to that used for the 11-year variation. Results thereby obtained are shown in Fig. 38, in comparison with that of the 11-year variation. There appears no significant difference in fractional decreases between both phenomena.

* The average atmospheric depth is 760 g/cm^2 for the mountain stations.

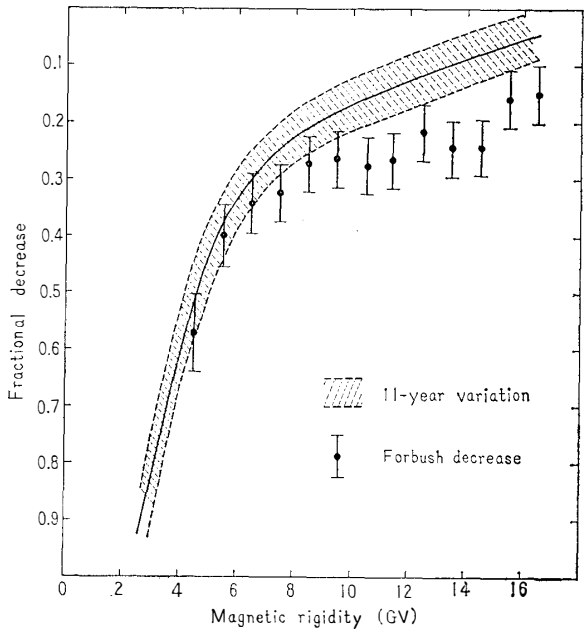

Fig. 38. Comparison between fractional decreases of the 11-year variation during 1954–1959 and the FORBUSH *decrease of July, 1959 as a function of the threshold rigidities.*

This suggests that both phenomena may be caused by a similar fashion of modulation mechanism, excepting the difference in time constant. Each of physical properties of the magnetic scattering center in the interplanetary space, such as dimension, life, and field strength, would be probably related to the respective magnitude and persistency of both intensity variations. Also, such physical states seem to be not always the same throughout all of the FORBUSH events. In other words, it may be possible from individual observation results of FORBUSH events to clarify the physical nature of the respective magnetic irregularities by which the FORBUSH event was caused.

2.7.2. Solar proton event of February 23, 1956

The intensity *versus* rigidity diagram of the greatest recorded solar proton event, that of February 23, 1956, is shown in Fig. 39 using both the T-values (with $N=5$ for calculation of the penumbral effect) and the QW-values. The amounts of intensity enhancements at individual stations are taken from QUENBY and WENK's diagram (1962). Of particular interest are three stations: Mexico City, Mt. Norikura and Huancayo. It is clear from both the curve for neutron monitors and the curve for ion chambers in Fig. 39, where a straight line in the region above 5 GV can be fitted much better for the case of the T-values than for the QW-values. In addition, Table 14 gives the r. m. s. deviations, in percentage rigidity, of the individual points from the best-fit curves using a linear relation above 5 GV and a parabolic curve below 5 GV. Table 14 also gives the r. m. s. deviation, in percentage, of the computation error included in the T-values, assuming is to be 0.1 GV. Since the r. m. s. deviations of the T-values are smaller than the QW-values and yet close to those of the 0.1 GV error, it is concluded

Table 14. The r. m. s. deviation in percentage of the threshold rigidity for solar proton event of February 23, 1956.

Threshold rigidity	Neutron	Ion-chamber
QUENBY and WENK	3.5% (14 stations)	4.4% (11 stations)
Trajectory	2.3 (9 stations)	1.7 (6 stations)
0.1 GV computation error	1.9	1.5

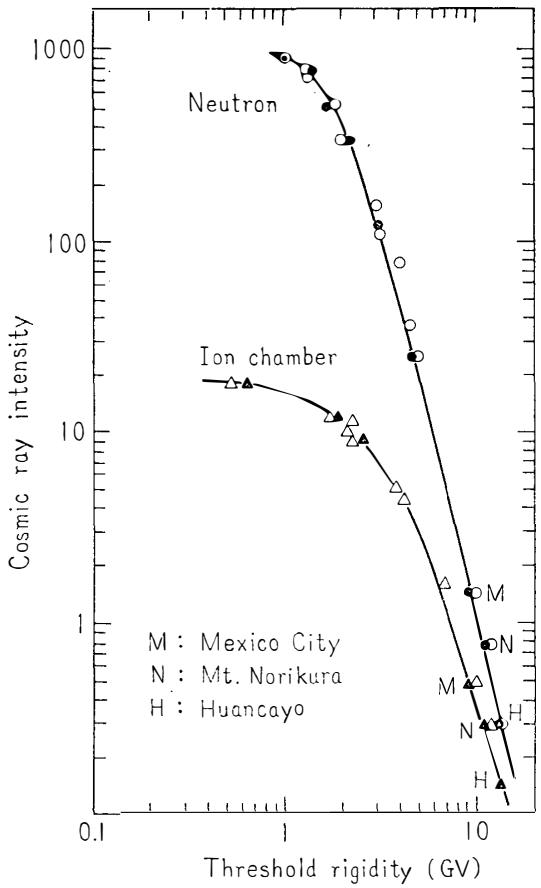

Fig. 39. Percentage increase for the solar event of February 23, 1956, for neutron monitors and ion chambers, as a function of the threshold rigidities. Marks ● and ▲ correspond to the trajectory-computed values, while ○ and △ are for the QUENBY and WENK's values.

that they can be attributed mainly to the computation error itself.

2. 8. Concluding remarks

The typical phenomena representing the geomagnetic effect of cosmic rays, *i. e.*, the cosmic-ray equator, the latitude knee and the rigidity, have been investigated in terms of the 11-year solar cycle. The position of the cosmic-ray equator at 110°E obtained from the SOYA surveys has remained almost constant during 1956–1962, though a small seasonal shift was found. Thus it is concluded that the cosmic-ray equator could be caused only by the influence of the earth's magnetic field and that it has no connection with the solar cycle modulation. An unexpected fact as to the position of the cosmic ray equator is a probable difference between the sea level and the airplane altitude results. It is a slight southward shift of the sea level equator from the high altitude one. No interpretation could be given of this discrepancy. On the other hand, the position of the latitude knee was modulated systematically with a yearly change of solar activity, as revealed by the hysteresis effect which

means a definite time lag of the long term variation in low energy portion of cosmic rays from that in solar activity. Namely, the solar modulation of the latitude knee is apparent not only in high altitudes but also at sea level, indicating the displacement from about 1 GV at the solar minimum to about 3 GV at the solar maximum.

The response function, which is an important character necessary for conversion from the observed sea level spectrum into the primary spectrum, was determined from latitude surveys at almost one year intervals during 1956–62. From comparisons among the response functions in different times, the 11-year intensity variation as a function of rigidity was deduced, and then compared with those obtained using neutron monitor data from a number of fixed stations at sea level. As a result, the difference of the rigidity spectrum between the ascending and the descending phases of the solar cycle was demonstrated, and also relative superiority and general availability of the response function were established in comparison with that based on station data. Furthermore, it was shown that the 11-year variation of the response curve is in good agreement with predictions by PARKER's solar wind modulation theory.

Last, actual applications of the trajectory-computed threshold rigidities and the response functions were made for a few special cosmic ray events. Results obtained, too, proved their general excellency. Particularly in the FORBUSH event of July, 1959, it was found that this event may have been caused by the solar wind modulation, as in the case of the 11-year variation of cosmic ray intensity.

General Concluding Remarks

Since the starting of measurements of the cosmic ray neutron intensisy as an indicator for the primary cosmic ray modulations, a number of latitude surveys have been carried out on board. The observed counting rate of the neutron intensity was less than 15,000 throughout all the surveys. Hence, it seems to be of importance for further investigations to consider both the merit and the limitation of the measurement associated with this order of accuracy. The presently available experimental results gave abundant evidences to show that the threshold rigidity determined by trajectory calculations is the best of all the threshold rigidities obtained so far. But simultaneously, they showed that there remains ultimately the uncertainty of less than 0.3 GV for the threshold rigidity. Three origins could be supposed to account for the uncertainty: 1) effects of the obliquely incident particles on the vertical threshold rigidity, 2) reliability of the geomagnetic field simulations adopted for the calculations and 3) ambiguities in the penumbral effect, or, errors introduced in the conversion process of the complexity of the penumbral region into a simple idea of cutoff. Though the present threshold rigidities must be revised further by taking these causes into account, the statistical accuracy of the measuremets performed up to now are not always good enough to check each of three causes quantitatively. If the ship can stay in an interesting place for a time, it would be possible to improve the statistical accuracy. In such case, however, other systematic errors will be inevitable due to the long term variation of the intensity level or due to incomplete pressure corrections. This may be the limitation of this sort of experiment.

It was proved that the present response functions are sufficiently valid for studies of the various intensity variation phenomena as observed at fixed stations, even if the above-mentioned uncertainties were involved fully. After all, the accuracy required for the response function is always in competition with that of the station data. Since the counting rate of the recently developed neutron monitor, NM-64, is at least one order greater than in the conventional monitor, it will be necessary to improve the experimental equipment for latitude surveys in order to deduce the corresponding response functions with better accuracy. In addition to the extension of the detector area, two important points to be improved are proposed as follows. One is the problem of neutron multi-

plicities arising in both the monitor pile and the atmosphere. As the number of the multiplicities depends upon the energy of the primary particles from which multiple neutrons are detected by the monitor, a kind of spectroscopic study becomes possible by the measurement of the incident particles responsible for each of different multiplicities. This also will be related to a problem of the fractional contribution of the extensive air shower into the multiple neutrons as detectable in the sea-level neutron monitor. Another problem is the experimental technique to measure the true barometric pressure on board. The barometric pressure is, in general, highly sensitive to the change in wind velocity. Consequently, the observed intensity of the nucleon component having a relatively large pressure coefficient should be disturbed considerably by strong wind, particularly on the ship. Furthermore, it is of course that the latitude dependence of the pressure coefficient has to be taken into account as well as its solar cycle modulation.

As for the 11-year variation of the sea-level latitude effect, it is necessary to compare and weigh its physical significance with the high altitude measurements by means of space vehicles. The essential difference between both measurements at different heights is that lower rigidity particles, less than 1 GV, and heavy nuclei components are detectable at high altitudes. Enhanced solar modulations would be expected for these particles and particularly a proton-helium ratio in flux gives the most decisive criterion for determining which theoretical modulation model is correct. The sea-level data seems to be rather inadequate to judge the suitability of the model, but it is believed that the exact determination of the response curve every year is still valid for studies of fine structures of time variations such as the hysteresis effect.

In addition to the present research objects, we would like to propose further experimental programs suitable for latitude surveys.

A). Latitude effect of total ionizing component

In all of the past measurements of the ionizing component, the absorber of 10 cm Pb was always used to remove the soft component. However, it is a question whether or not this sort of absorber is necessary for the counter telescope protected from natural background radiations by the coincidence method. A considerable loss of the absolute counting rate due to the lead absorber is very serious from a statistical standpoint. Since the actual response function of the total ionizing component is still unknown, the latitude survey for it will be desired in parallel with that for the muon component.

B). Latitude survey by means of undersea telescope

An aim of this experiment is to determine the threshold water depth at which the latitude effect just disappears for the muon component. If a series of intensity-depth measurements are carried out in different latitudes, the latitude dependence with water depth thereby obtained shall be useful for investigations of the atmospheric temperature effect and time variations of the ioniz-

ing component as observed at underground.

Furthermore, in case of the latitude survey by means of the high counting equipment, it probably would be necessary for the determination of the threshold rigidity to take into account the influence of time perturbations of the geomagnetic field effective to cosmic radiations. Possible modulations of the threshold rigidity may be arised from the following origins: the geomagnetic storm, and the asymmetry of the magnetospheric cavity against the earth's axis. Consequently, the latitude survey with better accuracy will facilitate the study of these physical properties.

Acknowledgements

The author wishes to express his hearty thanks to Dr. Y. MIYAZAKI and Prof. T. NAGATA for their constant interest and encouragement since the beginning of the Japanese Antarctic Research Expedition. He cordially thanks Dr. I. KONDO, University of Nagoya, for his valuable discussions and comments throughout the laborious machine computations. He also wishes to thank Prof. J. A. SIMPSON, University of Chicago, U. S. A., and Dr. H. CARMICHAEL, Atomic Energy of Canada Limited, Canada, who kindly provided the author with accommodation for utilizing their computation facilities. The author acknowledges fruitful discussions and kind assistances given by all colleagues in the cosmic ray laboratory, the Institute of Physical and Chemical Research, during the whole expedition period. Finally, the observers engaged in cosmic ray measurements aboard the SOYA were as follows:

SOYA-I	1956–57	M. KODAMA
SOYA-II	1958–59	S. FUKUSHIMA, deceased (Inst. Phys. Chem. Res.)
		T. KITAMURA (University of Kyoto)
SOYA-III	1959–60	S. FUKUSHIMA, deceased
		T. NAKAMURA (Tokyo Astro. Obs.)
SOYA-IIV	1960–61	T. MAKINO (University of Nagoya)
SOYA-V	1961–62	M. KODAMA

Many thanks are due to the late Mr. S. FUKUSHIMA, Drs. T. KITAMURA, T. NAKAMURA, and T. MAKINO, for their successful cooperations, particularly due to Mr. S. FUKUSHIMA who was lost in the vicinity of Syowa Station, Antarctica, on October 17, 1960, and found dead on February 10, 1968.

References

BACHELET, F., P. BALATA and N. IUCCI (1965): Some properties of the radiation recorded by the IGY cosmic ray neutron monitors in the lower atmosphere. Nuovo Cim., **40**, 250–260.

BARTELS, J. (1936): The eccentric dipole approximation to the earth's field. Terr. Magn. Atmos. Elect., **41**, 225–250.

CAIN, J. C., D. C. JENSEN, W. E. DANIELS, and S. HENDRICKS, (1964): American Geophys. Union Conf., Washington.

CARMICHAEL, H., M. BERCOVITCH, J. F. STELJES and M. MADIGIN (1965): Latitude survey in North America. Proc. Int. Conf. Cosmic Rays, London, **1**, 553–555.

CHAPMAN, S., and J. BARTELS (1951): Geomagnetism, **2**, Oxford Univ. Press, 606–637.

CHERNOSKY, E. J., J. M. COLLINS and M. P. HAGAN (1964): Equatorial loci of the earth's magnetic field and cosmic ray parameters. Pap. Air Force Camb. Res. Lab., **5**, 1–15.

COXELL, H., M. A. POMERANTZ and S. P. AGARWAL (1966): Survey of cosmic-ray intensity in the lower atmosphere. J. Geophys. Res., **71**, 143–154.

DORMAN, L. I. (1960): On the theory of the modulation of cosmic rays by the solar wind. Proc. Int. Conf. Cosmic Rays, Moscow, **4**, 320–329.

DORMAN, L. I. (1963): Progress in elementary particles and cosmic ray physics, **7**, North-Holland Publ.

EHMERT, A. (1960): On the modulation of the primary cosmic ray spectrum by solar activity. Proc. Int. Conf. Cosmic Rays, Moscow, **4**, 142–148.

EHMERT, A. (1962): Cosmic ray modulation and geomagnetism. J. Phys. Soc. Japan, **17**, (Suppl. A-II), 416–418.

ELLIOT, H. and J. J. QUENBY (1959): The samoan artificial aurora. Nature, **183**, 810.

ELLIOT, H., R. J. HYNDS, J. J. QUENBY, and G. J. WENK (1960): The cosmic ray time variation and the solar magnetic field. Proc. Int. Conf. Cosmic Rays, Moscow, **4**, 311–319.

FENTON, A. G., K. B. FENTON and D. C. Rose (1958): The variation of sea level cosmic ray intensity between 1954 and 1957. Can. J. Phys., **36**, 824–839.

FENTON, A. G., K. G. McCRACKEN, D. C. ROSE and B. G. WILSON (1959): Transient decrease in cosmic ray intensity during the period October 1956 to January 1958. Can. J. Phys., **37**, 569–578.

FINCH, H. P. and B. R. LEATON (1957): The earth's main magnetic field-epoch 1955. 0. Mon. Not. R. Astr. Soc., Geophys. Suppl., **7**, 314–317.

FORBUSH, S. E. (1954): World-wide cosmic ray variations 1937–1952. J. Geophys. Res., **59**, 525–542.

FORBUSH, S. E. (1958): Cosmic ray intensity during two solar cycles. J. Geophys. Res., **63**, 651–669.

FREON, A. and K. G. McCRACKEN (1962): A note on the vertical cutoff rigidities of cosmic rays in the geomagnetic field. J. Geophys. Res., **67**, 888–890.

FUKUSHIMA, S. and M. KODAMA (1961): Solar modulation effect on the latitude dependence in cosmic ray intensity. Sci. Pap. Inst. Phys. Chem. Res., **55**, 37–41.

FUKUSHIMA, S., M. KODAMA, T. MAKINO and MIYAZAKI (1964): Results of cosmic ray surveys between Japan and the Antarctic during 1956–1962. Antarctic Rec., **20**, 27–52.

GILL, S. P. (1951): A process for the step by step integration of differential equations in an automatic digital computing machine. Proc. Camb. Phil. Soc., **47**, 96–108.

GLOECKLER, G. and J. R. JOKIPII (1966): Low-energy cosmic-ray modulation related to observed

interplanetary magnetic field irregularities. Phys. Rev., **17**, 203–207.

GRIFFITHS, W. K., C. J. HATTON, P. Ryder and C. V. HARMAN (1966): The variation of the barometric coefficient of the Leeds neutron monitor during the solar cycle 1954–1965. J. Geophys. Res., **71**, 1895–1898.

HAKURA, Y. (1964): Patterns of polar cap blackouts drawn in geomagnetic coordinates corrected by the higher terms of spherical harmonic development. Rep. Ionosp. Space Res. Japan, **18**, 345–365.

HAKURA, Y. (1965): Tables and maps of geomagnetic coordinates corrected by the higher order spherical harmonic terms. Rep. Ionosph. Space Res. Japan, **19**, 121–157.

JENSEN, D. C. and W. A. WHITAKER, (1960): A spherical harmonic analysis of the geomagnetic field. J. Geophys. Res., **65**, 2500.

JENSEN, D. C. and J. C. CAIN (1962): An iterium geomagnetic field. J. Geophys. Res., **67**, 3568.

JORY, F. S. (1956): Influence of geomagnetic quadrupole fields upon cosmic-ray intensity. Phys. Rev., **102**, 1167–1173.

JORY, F. S. (1956): Selected cosmic-ray orbits in the earth's magnetic field. Phys. Rev., **103**, 1068–1075.

KATZ, L., P. MEYER and J. A. SIMPSON (1958): Further experiments concerning the geomagnetic field effective for cosmic rays. Nuovo Cim., **8**, 277–282.

KELLOGG, P. J. and M. SCHWARTZ (1959): Theoretical study of the cosmic ray equator. Nuovo Cim., **13**, 761–768.

KELLOGG, P. J. (1960): Calculations of cosmic-ray trajectories near the equator. J. Geophys. Res., **65**, 2701–2703.

KODAMA, M., I. KONDO and M. WADA (1957): Cut-off rigidities of cosmic-ray particles calculated for the eccentric dipole model of the earth's magnetic field. J. Scient. Res. Inst., Tokyo, **51**, 138–157.

KODAMA, M. (1960): Cosmic rays at sea level and the earth's magnetic field. Sci. Pap. Inst. Phys. Chem. Res., **54**, 20–42.

KODAMA, M. and M. WADA (1960): Intensity minimum in cosmic-ray neutrons during the International Geophysical Year. J. Geophys. Res., **65**, 2203–2205.

KODAMA, M., S. FUKUSHIMA and T. MAKINO (1962): Secular variation of the cosmic ray equator and the latitude knee at sea level. J. Phys. Soc. Japan, **17** (Suppl. A-II), 441–444.

KODAMA, M. (1963): Cosmic-ray latitude knee around Cape Town. Nature, **198**, 472–474.

KODAMA, M. (1965): Trajectory-computed vertical threshold rigidities for 85 neutron monitor stations. Can. J. Phys., **43**, 836–848.

KODAMA, M. and T. OHUCHI: Latitude survey of the neutron multiplicity using a shipborne NM-64 neutron monitor. Proc. Int. Conf. Cosmic Rays, Calgary, in press.

KODAMA, M. and A. INOUE; to be published.

KONDO, I., M. KODAMA and T. MAKINO (1963): Changes in the primary cosmic ray rigidity spectrum over a solar cycle as derived from latitude effect. Proc. Int. Conf. Cosmic Rays, Jaipur, **2**, 383–385.

KONDO, I., M. KODAMA and T. MAKINO (1963): Cosmic ray threshold rigidities determined from trajectory calculations. Proc. Int. Conf. Cosmic Rays, Jaipur, **2**, 386–389.

KONDO, I. and M. KODAMA (1965): Geographic distribution of vertical cosmic ray threshold rigidities. Proc. Int. Conf. Cosmic Rays, London, **1**, 558–563.

KONDO, I. (1966): Private communication.

LOCKWOOD, J. A. (1958): Variations in the cosmic-ray nucleonic intensity. Phys. Rev., **112**, 1750–1758.

LOCKWOOD, J. A. (1960): On the long-term variation in the cosmic radiation. J. Geophys. Res., **65**, 19–25.

MAKINO, T. (1963): On the cosmic ray cutoff rigidities and the earth's magnetic field. Rep. Ionosph. Space Res. Japan, **17**, 173–186.

MATHEWS, T. and M. KODAMA (1964): Magnetic rigidity dependence of eleven-year variation in cosmic ray intensity. J. Geophys. Res., **69**, 4429–4434.

MCCRACKEN, K. G. and N. R. PARSONS (1958): Unusual cosmic-ray intensity fluctuations observed at southern stations during October 21–24, 1957. Phys. Rev., **112**, 1798–1801.

MCCRACKEN, K. G. (1960): Energy dependence of transient changes in the primary cosmic-ray spectrum. Phys. Rev., **117**, 1570–1579.

MCCRACKEN, K. G., U. R. RAO and M. A. SHEA (1962): The trajectories of cosmic rays in a high degree simulation of the geomagnetic field. Mass. Tech. Rept., **77**, 1–83.

MEYER, P. and J. A. SIMPSON (1957); Changes in the low-energy particles cutoff and primary spectrum of cosmic rays. Phys. Rev., **106**, 568–571.

NAGASHIMA, K., S. P. DUGGAL and M. A. POMERANTZ (1966): Long term modulation of cosmic ray intensity. Planet. Space Sci., **14**, 177–206, 1966.

NEHER, H. V. and H. R. Anderson (1960): The knee of the latitude curve at balloon altitude. Proc. Int. Conf. Cosmic Rays, Moscow, **4**, 104–107.

OGUTI, T. and M. KODAMA (1959): Difference between cosmic-ray equator and the geomagnetic dip equator. Nature, **183**, 103.

PARKER, E. N. (1958): Cosmic-ray modulation by solar wind. Phys. Rev., **110**, 1445–1449.

PARKER, E. N. (1963): Interplanetary dynamical processes, Interscience.

du PLOOY, N. F., G. J. KUHN, J. P. MAREE, P. H. STOKER and A. J. VAN DER WALT (1963): Cosmic-ray intensity distributions at 640 grams per square centimeter atmospheric depth around Cape Town. J. Geophys. Res., **68**, 3123–3130.

POMERANTZ, M. A., V. R. POTNIS and A. E. SANDSTRÖM (1960): The cosmic-ray equator and the earth's magnetic field. J. Geophys. Res., **65**, 3539–3543.

POMERANTZ, M. A., A. E. SANDRTRÖM, V. R. POTNIS and D. C. ROSE (1960): Solar disturbances and the cosmic ray equator. Tellus, **12**, 231–235.

POMERANTZ, M. A. and S. P. AGARWAL (1962): Spatial distribution of cosmic ray intensity and geomagnetic theory. Phil. Mag., **7**, 1503–1511.

POMERANTZ, M. A. (1965): Private communication.

QUENBY, J. J. and W. R. WEBBER (1959): Cosmic-ray cutoff rigidities and the earth's magnetic field. Phil. Mag., **4**, 90–113.

QUENBY, J. J. and G. J. WENK (1962): Cosmic ray threshold rigidities and the earth's magnetic field. Phil. Mag., **7**, 1457–1485.

ROSE, D. C., K. B. FENTON, J. KATZMAN and J. A. SIMPSON (1956): Latitude effect of the cosmic ray nucleon and meson components at sea level from the Arctic to the Antarctic. Can. J. Phys., **34**, 968–984.

SCHWARTZ, M. (1959): Penumbra and simple shadow cone of cosmic radiation. Nuovo Cim. Suppl., **11**, 27–59.

SHEA, M. A., D. F. SMART and J. F. KENNEY (1964): The cosmic-ray equator at 170° west longitude. J. Geophys. Res., **69**, 4162–4165.

SHEA, M. A., D. F. SMART and K. G. MCCRACKEN (1965a): A study of vertically incident cosmic-ray trajectories using sixth-degree simulations of the geomagnetic field. Rep. Air Force Camb. Res. Lab., AFCRL-65-705.

SHEA, M. A., D. F. SMART, and K. G. MCCRACKEN (1965b): A study of vertical cutoff rigidi-

ties using sixth degree simulations of the geomagnetic field. J. Geophys. Res., **70**, 4117–4130.

SHEA, M. A., and D. F. SMART (1967): Worldwide trajectory-derived vertical cutoff rigidities and their application to experimental measurements. J. Geophys. Res., **72**, 2021–2027.

SIMPSON. J. A. and W. C. FAGOT (1953): Properties of the low energy nucleonic component at large atmospheric depths. Phys. Rev., **90**, 1068–1072.

SIMPSON, J. A. (1956); American Geophys. Union Symposium, Washington.

SIMPSON, J. A., K. B. FENTON, J. KATZMAN and D. C. ROSE (1956): Effective geomagnetic equator for cosmic radiation. Phys. Rev., **102**, 1648–1653.

Simpson, J. A., F. JORY and M. PYKA (1956): On driving geomagnetic dipole-field coordinates from cosmic ray observations. J. Geophys. Res., **61**, 11–22.

SIMPSON, J. A. (1962): Recent investigations of the low energy cosmic and solar particle radiations, Seminar on the problem of cosmic radiation in interplanetary space. Vaticana, 323–343.

SIMPSON, J. A. *et al.* (1963): Unpublished data for 1955–56, 1956–57. Antarctic expeditions by University of Chicago.

SKORKA, S. (1958): Breiteneffekt der Nukleonen und Mesonenkomponente der Ultrastrahlung in Meereshöhe im Indischen und Atlantischen Ozean. Z. Phys., **151**, 630–645.

STONE, E. C. (1963): The physical significance and application of L, B_0, and R to geomagnetically trapped particles. J. Geophys. Res., **68**, 4157–4166.

STOREY, J. R. (1959): Cosmic-ray latitude survey along 145°E longitude using an airborne neutron monitor. Phys. Rev., **113**, 297–301.

WEBBER, W. R. (1962): Progress in elementary particles and cosmic ray physics, **6**, North-Holland Publ.

WINCKLER, J. R. (1962): Geomagnetic and interplanetary effects on solar cosmic rays. J. Phys. Soc. Japan, **17** (Suppl. A-II), 353–360.

(*Manuscript received March 6, 1968*)